Paraconductivity of pseudogapped superconductors

Igor Poboiko[1,2,3] and Mikhail Feigel'man[3,2]
[1]*Skolkovo Institute of Science and Technology, Moscow 143026, Russia*
[2]*National Research University "Higher School of Economics," Moscow 101000, Russia*
[3]*L. D. Landau Institute for Theoretical Physics, Chernogolovka 142432, Moscow region, Russia*

(Received 21 October 2017; revised manuscript received 26 December 2017; published 10 January 2018)

We calculate Aslamazov-Larkin (AL) paraconductity $\sigma_{\rm AL}(T)$ for a model of strongly disordered superconductors (dimensions $d = 2,3$) with a large pseudogap whose magnitude strongly exceeds transition temperature T_c. We show that, within Gaussian approximation over Cooper-pair fluctuations, paraconductivity is just twice larger that the classical AL result at the same $\epsilon = (T - T_c)/T_c$. Upon decreasing ϵ, Gaussian approximation is violated due to local fluctuations of pairing fields that become relevant at $\epsilon \leqslant \epsilon_1 \ll 1$. Characteristic scale ϵ_1 is much larger than the width ϵ_2 of the thermodynamical critical region, that is determined via the Ginzburg criterion, $\epsilon_2 \approx \epsilon_1^d$. We argue that in the intermediate region $\epsilon_2 \leqslant \epsilon \leqslant \epsilon_1$, paraconductivity follows the same AL power law, albeit with another (yet unknown) numerical prefactor. At further decrease of the temperature, all kinds of fluctuational corrections become strong at $\epsilon \leqslant \epsilon_2$; in particular, conductivity occurs to be strongly inhomogeneous in real space.

DOI: 10.1103/PhysRevB.97.014506

I. INTRODUCTION

Strongly disordered superconductors near quantum phase transition into an insulator state have attracted great interest during the last years [1–13]. On the experimental side [5–14], new methods which became available, such as low-temperature scanning tunneling spectroscopy, make it possible to study properties of the superconducting state locally with a nanometer-scale resolution. As a result [5,6], an existence of a strong density-of-states (DOS) suppression at temperatures much above the superconducting transition T_c was demonstrated. Such a phenomenon is called *pseudogap*, in some rough analogy to the phenomenon known for underdoped high-T_c oxide superconductors; however, the origin of pseudogap in usual strongly disordered superconductors like InO_x (see Refs. [1,2]), is unrelated to various courses of pseudogap origin, discussed in relation to a high-temperature superconductor (HTSC). A detailed semiquantitative theory of superconductivity, starting from BCS-type model with localized single-electron states [near three-dimensional (3D) Anderson localization transition] was developed in Refs. [1,2], elaborating an approach proposed originally in [15] and developed numerically in [16].

One of the most general phenomena inherent to disordered superconductors is known to be fluctuational conductivity (paraconductivity) predicted long ago by Aslamazov and Larkin [17]. It is due to appearance of fluctuational (with finite lifetime) Cooper pairs at temperatures slightly above T_c. Aslamazov-Larkin (AL) paraconductivity is especially universal in two-dimensional (2D) superconductors, where additional conductance *per square* is

$$\sigma_{\rm AL}^{\square} = \frac{e^2}{16\hbar}\frac{T}{T - T_c}$$

independently of any microscopic parameters. This result is usually considered to be valid as long as $\sigma_{\rm AL}$ is much smaller than Drude conductance of the metal σ_0, i.e., at $\epsilon \equiv T/T_c - 1 \gg {\rm Gi} = e^2/16\hbar\sigma_0$, that is, in the region of Gaussian fluctuations. In bulk systems, paraconductivity is less singular, $\sigma_{\rm AL} \propto (T - T_c)^{-1/2}$.

More close to the transition point, within fluctuational region $\epsilon \leqslant {\rm Gi}$, interaction between superconducting fluctuations becomes important and results in the universal scaling behavior of thermodynamics quantities [18], that is determined exclusively by space dimensionality and order-parameter symmetry. In what concerns kinetic properties (such as conductivity), the situation is less clear. Reference [19] provided arguments in favor of the statement that paraconductivity is more sensitive to nonlinear effects and deviates from classical AL form already at $\epsilon \leqslant \sqrt{\rm Gi}$, that is, parametrically far from the scaling region. Basically, the arguments of Ref. [19] were based upon the suppression of the electron density of states (DOS) due to superconducting fluctuations: reduced DOS leads to suppression of the electron-electron inelastic rate; in turn, that leads to an increase of the order-parameter relaxation time $\tau_{\rm GL}$, with respect to its value known from the Gaussian approximation $\tau_{\rm GL}^{(0)} = \pi\hbar/8(T - T_c)$. Since paraconductivity $\sigma_{\rm AL}$ can be generally shown to be proportional to the product $T\tau_{\rm GL}$, the above consideration suggests its more singular behavior due to fluctuational suppression of the DOS. However, detailed calculations of the proposed effect were performed [19] for the case when strong depairing is present and the whole effect is anyway weak; it remained unclear if indeed temperature behavior of paraconductivity changes qualitatively in the range $\epsilon \leqslant \sqrt{\rm Gi}$.

In this paper, we provide an analysis of a similar problem from a different perspective. Namely, we consider a very strongly disordered superconductor with a well-developed pseudogap Δ_P. An existence of pseudogap Δ_P is due to (i) localized nature of single-electron eigenstates $\psi_i(\boldsymbol{r})$, and (ii) phonon-induced attraction between electrons which leads to formation of localized electron pairs (with opposite spins) populating eigenstates $\psi_i(\boldsymbol{r})$. The energy gain due to formation

of such a pair is Δ_P. Next, hybridization matrix elements J_{ij} provide virtual hopping of electron pairs between different localized eigenstates. If this hopping is sufficiently strong, a superconducting coherent state is formed below some critical temperature T_c (for detailed theory of pseudogapped superconductivity, see [2]).

Below we consider the case of Δ_P that is much larger than T_c, like it was found in InO_x thick films studied in Ref. [5]. In such a case, one may neglect, to a first approximation over $T_c/\Delta_P \ll 1$, the presence of single-electron states: the single-particle DOS will be set to zero. We will show, nevertheless, that the whole qualitative picture of critical fluctuations, including their dynamics, remains the same as for usual disordered superconductors, as long as we stick to the Gaussian fluctuation region. The major difference we found is that now $\tau_{GL}^{(0)} = \pi\hbar/4(T - T_c)$, i.e., twice larger than the result of the standard theory.

This result is valid as long as thermal fluctuations are weak and their interaction can be neglected. For such a region to exist at $\epsilon \leqslant 1$ in a pseudogapped superconductor, a special assumption is necessary; namely, we consider the model with interaction matrix elements J_{ij} possessing large coordination number $Z \gg 1$ for the relevant eigenstates which have eigenenergies $\varepsilon_i, \varepsilon_j$ located within about T_c from Fermi energy. The presence of large parameter Z allows us to derive a dynamical Ginzburg-Landau (GL) functional for superconducting fluctuations at T near T_c and to calculate paraconductivity at $\epsilon \geqslant \epsilon_1$, where explicit value of $\epsilon_1 \ll 1$ depends both on Z and on space dimensionality d (we consider $d = 2,3$). At smaller ϵ interaction between fluctuations becomes strong enough to affect kinetic coefficient of the Ginzburg-Landau functional, thus, the kinetic problem cannot be solved analytically; however, we provide some arguments in favor of the same type power-law singularity in paraconductivity $\sigma_{AL} \propto (T - T_c)^{(d-4)/2}$ to exist down to much smaller values of $\epsilon \geqslant \epsilon_2$. Here, ϵ_2 provides a boundary of the region where all thermodynamic fluctuational effects become strong, it is analogous to the Ginzburg parameter in the usual theory of second-order phase transitions; the important point is that $\epsilon_2 \ll \epsilon_1$ as long as $\epsilon_1 \ll 1$.

The rest of the paper is organized as follows: in Sec. II we formulate our model based upon Anderson pseudospin [20] representation of the even-only sector of BCS Hamiltonian for localized single-electron states; we provide initial mean-field-like analysis in Sec. II A and then in Sec. II B we develop Popov-Fedotov semionic diagrammatic technique that is convenient to treat long-range and long-time properties of the model near the critical point. Section III is devoted to the derivation of the dynamic Ginzburg-Landau functional and to the calculation of the paraconductivity within Gaussian approximation for 2D and 3D systems. In Sec. IV we analyze leading non-Gaussian corrections and estimate characteristic temperature scale ϵ_1; we find that it scales as $Z^{-1/2}$ and $Z^{-2/3}$ in 2D and 3D cases, correspondingly; we also analyze the effect of these non-Gaussian corrections upon dependence of σ_{AL} on ϵ. Then, in Sec. V we consider all other effects beyond the leading Gaussian approximation; these effects are (a) the lack of self-averaging due to strong spatial fluctuations of disorder, and (b) infra-red-dominated thermal fluctuations of collective modes. We show that corresponding reduced temperature scale $\epsilon_2 \propto 1/Z$ in the 2D model, and $\propto 1/Z^2$ in 3D; note that it is the same scaling as it is known for the Ginzburg number Gi in usual phase transition theory. Section VI contains our conclusions. Some technical details are presented in Appendices A, B, C, and D.

II. MODEL AND DIAGRAM TECHNIQUE

The starting point of our approach is representation of the *paired* electron system in terms of pseudospin operators introduced long ago by Anderson [20]:

$$S_i^- = a_{i\downarrow}a_{i\uparrow}, \quad S_i^+ = a_{i\uparrow}^\dagger a_{i\downarrow}^\dagger, \quad 2S_i^z = a_{i\uparrow}^\dagger a_{i\uparrow} + a_{i\downarrow}^\dagger a_{i\downarrow} - 1. \tag{1}$$

Here, operators $a_{i\uparrow}$ and $a_{i\downarrow}$ and, correspondingly, $a_{i\uparrow}^\dagger$ and $a_{i\downarrow}^\dagger$, represent electron annihilation (creation) operators for ith single-particle eigenstate $\psi_i(\boldsymbol{r})$ which are assumed to be localized. Then, operators S_i^α introduced in (1) obey standard spin-$\frac{1}{2}$ commutation relations. The Hilbert space spanned by the set of S_i^α operators constitutes a part of the whole Hilbert space of the electron system; namely, we omit the states with some eigenstates $\psi_i(\boldsymbol{r})$ to be single occupied. This is a reasonable approximation as long as two-electron local binding energy Δ_P is much larger than all energy/temperature scales relevant for the problem to be considered (see Ref. [2]).

The minimal Hamiltonian that describes development of superconducting correlations between localized electron pairs is of the form

$$H = -2\sum_i \varepsilon_i S_i^z - \frac{1}{2}\sum_{ij} J_{ij}(S_i^+ S_j^- + \text{H.c.}), \tag{2}$$

where ε_i are single-electron eigenvalues which are assumed to be distributed independently with the box distribution function $P(\varepsilon) = \frac{1}{2W}\theta(W - |\varepsilon|)$. The exact shape of the distribution function is important only for the T_c definition; as we will show below, the critical behavior near the transition (such as paraconductivity) depends only on the shape of the distribution function at $\varepsilon \lesssim |T - T_c|$. As long as density of states $\nu_0 = P(0)$ is finite, all the results will hold the same.

Matrix elements $J_{ij} \equiv J(\boldsymbol{r}_i - \boldsymbol{r}_j) \propto \int d^d r\, \psi_i^2(\boldsymbol{r})\psi_j^2(\boldsymbol{r})$ actually depend in nontrivial way on the distance $\boldsymbol{r} = \boldsymbol{r}_i - \boldsymbol{r}_j$ as well as on the energy difference $\varepsilon_i - \varepsilon_j$; to simplify the problem, we employ below a model where J_{ij} are assumed to have large radius $R \gg 1$, and its Fourier transform takes the form $J(\boldsymbol{p}) = J(1 - p^2R^2)$ in the long-wavelength limit. Here and thereafter we take the concentration of the localized states n to be unity, i.e., we measure all lengths in terms of $n^{-1/d}$. In that sense, $R \gg 1$ corresponds to large concentration, and all the summation over localized states $\sum_i f(\boldsymbol{r}_i)$ can be replaced by integration $\int d\boldsymbol{r}\, f(\boldsymbol{r})$. Also, we should note that J here corresponds to zero Fourier harmonic of $J(\boldsymbol{r})$, and can parametrically differ from *typical* value of $J_{ij} \sim J/R^d$.

It will be seen below that our major results rely upon the possibility to derive an effective dynamic Ginzburg-Landau theory valid at the temperatures close to T_c. In that respect, the neglect of the energy dependence of the matrix elements J_{ij} seems to be harmless, as long as effective number of neighbors Z is large. This condition $Z \gg 1$ is indeed crucial for our theory to be constructed. It is not evident that such a condition can be fulfilled within a microscopic model of superconductor

near localization threshold developed in Ref. [2]. However, we believe that the analysis provided below within the assumption of large Z is useful, in spite of the absence of microscopic justification of such a model at the present moment.

The disorder is assumed to be large, and the temperature is assumed to be small, so that $W \gg J \gg T$.

A. Mean field critical temperature and order parameter

The BCS order parameter, which is the anomalous average, corresponds to nonzero in-plane spin magnetization $\langle S_i^{x,y}\rangle$. The natural choice for the order parameter for the mean field treatment is thus the following:

$$\Phi_i^\alpha = \sum_j J_{ij}\langle S_j^\alpha\rangle, \quad \alpha = x,y \tag{3}$$

while the ordinary superconducting complex order parameter takes the form $\Delta = \Phi^x + i\Phi^y$.

In the mean field approximation, one decouples spins living in effective magnetic field created collectively by other spins:

$$H_{\rm MF} = -\sum_{i,\alpha} h_i^\alpha \sigma_i^\alpha, \tag{4}$$

with Pauli matrix $\sigma_i^\alpha = 2S_i^\alpha$ and effective magnetic field $\boldsymbol{h}_i = (\Phi_i^x, \Phi_i^y, \varepsilon_i)$. The Hamiltonian (4) yields trivial partition function for each spin $Z_i = 2\cosh(\beta|h_i|)$, with β being the inverse temperature $\beta = T^{-1}$. From this partition function we immediately extract the average magnetization $\langle S_i^\alpha\rangle = \frac{T}{2}\frac{\partial \ln Z_i}{\partial h_i^\alpha}$, which yields the following self-consistency equations:

$$\sum_j J_{ij}\eta_j\Phi_j^\alpha = \Phi_i^\alpha, \quad \eta_j = \frac{\tanh\beta\sqrt{\varepsilon_j^2+\Phi_j^2}}{2\sqrt{\varepsilon_j^2+\Phi_j^2}}. \tag{5}$$

Note that matrix $J_{ij}\eta_j$ entering these equations is non-Hermitian; however, it can be made Hermitian trivially by rescaling $\Phi_i \mapsto \Phi_i/\sqrt{\eta_i}$ yielding a new matrix $\sqrt{\eta_i\eta_j}J_{ij}$. These equations acquire a nontrivial solution if the matrix has a unity eigenvalue. The critical temperature T_c can be defined as the highest temperature that is consistent with the same condition for $\boldsymbol{\Phi} = 0$.

Under the assumption of a very large interaction radius R, one can simply average all η_i over ε_i and assume a homogeneous order parameter $\Phi_i^\alpha \equiv \Phi^\alpha$. These simplifications lead to the self-consistency equation, which is nearly equivalent to the BCS one:

$$1 = \frac{J}{2}\int d\varepsilon\, P(\varepsilon)\frac{\tanh\left(\beta\sqrt{\varepsilon^2+\boldsymbol{\Phi}^2}\right)}{\sqrt{\varepsilon^2+\boldsymbol{\Phi}^2}}. \tag{6}$$

For the box-shaped distribution $P(\varepsilon)$, the critical temperature that follows from this equation reads as

$$T_c = \frac{4e^\gamma}{\pi}We^{-1/g}, \quad g = \nu_0 J. \tag{7}$$

Here, $\gamma \approx 0.577$ is Euler's constant. The parametric dependence $T_c \sim We^{-1/g}$ is not sensitive to the exact shape of the distribution function, only the numerical prefactor is. Relevant parameters of the distribution function are nonzero DOS $\nu_0 = P(0)$ and a typical width W.

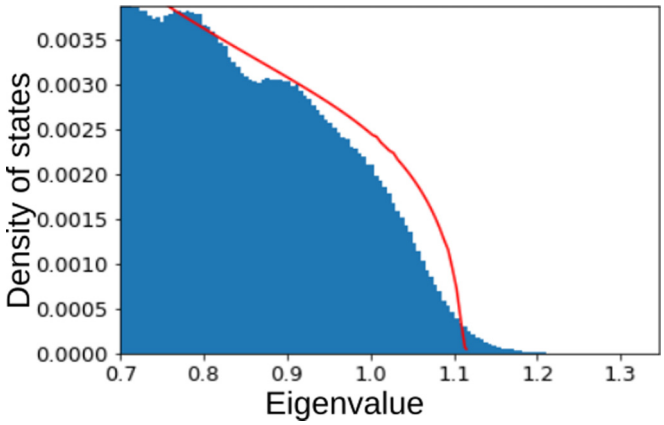

FIG. 1. DOS of the random matrix $J_{ij}\sqrt{\eta_i\eta_j}$ for 200×200 system with the following parameters: $R = 5$, $J = 1$, $W = 3$, $\beta \approx \beta_c \approx 60$. Red curve: analytical fit given by SCBA approximation (see Appendix A for more details).

Note the absence of factor 2 in denominator in the argument of tanh in Eq. (6); this is due to the absence of odd-electron states in the Hilbert space of our model. In result, the value of T_c is twice larger than in the BCS theory.

The value of the order parameter at $T = 0$ is given exactly by the standard BCS formula

$$\Phi(0) = 2We^{-1/g}. \tag{8}$$

Equation (6) is exactly valid in the limit of $R \to \infty$ only. For a finite R, in order to find T_c, one should consider actual matrix $J_{ij}\sqrt{\eta_i\eta_j}$ for a given realization of $\{\varepsilon_i\}$ and look for β that corresponds to its highest eigenvalue equal to 1. Below we provide major results of the corresponding numerical analysis (the details are presented in Appendix A).

Taking into account the large yet finite R leads to the shift of the criterion for superconductivity from the value given by (7) to the larger temperatures. Typical behavior of the DOS at large R obtained by means of numerical diagonalization and disorder averaging is shown on Fig. 1. The "main body" of the DOS fits reasonably well with the one predicted by the self-consistent Born approximation (SCBA) developed in the Appendix A, and the width of the exponential tail is proportional to the Ginzburg number $\mathrm{Gi} \sim \rho^{2/(4-d)}$ with ρ given by (38) and (39). Oscillatory behavior is an artifact caused by finite size of the system.

B. Semionic description and Keldysh diagram technique

In order to study the dynamical properties of the order parameter and develop a diagram technique, we choose the Fedotov-Popov representation for spin-$\frac{1}{2}$ operators [21,22]. Namely, for each spin we introduce a two-component spinor $\psi = (\psi_\uparrow, \psi_\downarrow)$ describing a pair of fermions (called semions for the reason that will become clear soon), and represent spin operators in terms of semions [below $\hat\sigma^\alpha$ is the set of Pauli matrices acting in the $(\uparrow,\downarrow)$ space]:

$$S_i^\alpha = \tfrac{1}{2}\psi_i^\dagger\hat\sigma^\alpha\psi_i. \tag{9}$$

The physical subspace contains two states and corresponds to the presence of exactly one semion: $\psi_\alpha^\dagger\psi_\alpha = 1$; in order to get

rid of two extra (unphysical) degrees of freedom, one should introduce an imaginary chemical potential $\mu = -\frac{i}{2}\pi T$ for the semions [21]. In the imaginary-time Matsubara representation, such an addition to the chemical potential is equivalent to the additional phase shift equal to $\pm\pi/2$ for fermionic fields translation over period along the imaginary-time axis: $\psi_\alpha(\tau + \beta) = (\pm i)\psi_\alpha(\tau)$, thus, these modified fermions were coined "semions."

The Hamiltonian (2) expressed in terms of semionic degrees of freedom reads as

$$H = -\sum_i \varepsilon_i \psi_i^\dagger \hat\sigma^z \psi_i - \frac{1}{4}\sum_{ij,\alpha}(\psi_i^\dagger \hat\sigma^\alpha \psi_i) J_{ij} (\psi_j^\dagger \hat\sigma^\alpha \psi_j). \quad (10)$$

This expression for the Hamiltonian allows us to build a Keldysh diagram technique for calculation of spin-spin–correlation functions. After decoupling the four-semion interaction using the Hubbard-Stratanovich order-parameter field Φ (see Appendix B for the detailed derivation), we arrive at the following Keldysh action describing semionic as well as order-parameter degrees of freedom:

$$iS[\bar\psi,\psi,\Phi] = i\int dt\left[-\Phi^\alpha \hat J^{-1}\check\tau_x \Phi^\alpha + \bar\psi\left(\hat G^{-1} + \frac{1}{\sqrt{2}}\check\Gamma_\mu \hat\sigma^\alpha \Phi_\mu^\alpha\right)\psi\right]. \quad (11)$$

Here, index $\mu \in \{cl,q\}$ denotes "classical" and "quantum" Keldysh components; vertices $\check\Gamma_{cl} = \check\tau_0$, $\check\Gamma_q = \check\tau_x$ with $\check\tau_\alpha$ being Pauli matrices acting in Keldysh space; and $\hat G^{-1} = i\partial_t + \varepsilon_i\hat\sigma^z$ is a matrix, diagonal in the real space.

The quadratic part of the action is used to build the following "bare" propagators for the order parameter $L^{\alpha\beta}(t-t') = i\langle\Phi^\alpha(t)\Phi^\beta(t')\rangle$ [which appears to be diagonal in spin space $(L^{(0)})^{\alpha\beta} = \delta^{\alpha\beta}L^{(0)}$]:

$$L^{(0)}_{R/A}(\omega,\boldsymbol{q}) = J(\boldsymbol{q})/2, \quad (12)$$

and for the semions $G_{\sigma\sigma'}(t-t') = -i\langle\psi_\sigma(t)\psi^\dagger_{\sigma'}(t')\rangle$ (with $\sigma,\sigma' \in \{\uparrow,\downarrow\}$):

$$\hat G^{(0)}_{R/A}(\omega) = \begin{pmatrix}(\omega \pm i\gamma + \varepsilon)^{-1} & 0\\ 0 & (\omega \pm i\gamma - \varepsilon)^{-1}\end{pmatrix} = \hat{\mathbb{P}}^\uparrow G^\uparrow_{R/A}(\omega) + \hat{\mathbb{P}}^\downarrow G^\downarrow_{R/A}(\omega). \quad (13)$$

Here, $\hat{\mathbb{P}}^{\uparrow,\downarrow} = \frac{1}{2}(1 \pm \hat\sigma^z)$ are the projectors onto the z axis. The imaginary part γ should be taken positive infinitesimal.

Finally, in the equilibrium, the standard Keldysh relation holds:

$$L_K(\omega) = \mathfrak{B}(\omega)\Delta L(\omega), \quad \mathfrak{B}(\omega) = \coth\frac{\beta\omega}{2}, \quad (14)$$

and

$$G_K(\omega) = \mathfrak{F}(\omega)\Delta G(\omega), \quad \text{with}$$
$$\mathfrak{F}(\omega) = \mathfrak{f}(\omega) - \frac{i}{\cosh\frac{\beta\omega}{2}}, \quad \mathfrak{f}(\omega) = \tanh\beta\omega, \quad (15)$$

where the shorthand notation $\Delta(\dots) = (\dots)_R - (\dots)_A$ is introduced. The only modification is that semions acquire an imaginary part in their distribution function, which is due to the imaginary chemical potential $\mu = -i\pi T/2$. That does not produce any problem since semions themselves do not correspond to any physical degrees of freedom, while original spins do.

Below we will use the developed diagram technique in order to calculate the order-parameter correlation function $L(\omega,\boldsymbol{q})$ above the transition temperature, but in its close vicinity, where critical slowing down takes place.

C. Electric current

Anderson pseudospin operators $S_i^\pm$ create and annihilate pair of electrons on site i. The electromagnetic gauge transformation thus acts as U(1) rotation on the spin operators $S_i^\pm \mapsto S_i^\pm e^{\pm 2ie\alpha(\boldsymbol{r}_i)}$ (with e being electron charge, while speed of light is taken $c = 1$). Accompanied by the gauge transformation for the vector potential $\boldsymbol{A}(\boldsymbol{r}) \mapsto \boldsymbol{A}(\boldsymbol{r}) - \nabla\alpha$ this should leave the action (11) unchanged.

Real space enters problem via the $\hat J = J(\hat p = -i\nabla)$ matrix. The gauge field $\boldsymbol{A}$ thus enters the action by replacing momentum by the "covariant derivative" $\hat{\boldsymbol{P}} = \hat{\boldsymbol{p}} - 2e\boldsymbol{A}\hat\sigma^y$. The long-wavelength limit corresponds to $\hat J^{-1} \equiv \hat J^{-1}(\hat{\boldsymbol{P}}) \approx J^{-1}(1 + \hat{\boldsymbol{P}}^2R^2)$.

The electrical current induced by Cooper pairs can be extracted from the action using the following relation:

$$\boldsymbol{j} = \frac{\delta S}{\delta \boldsymbol{A}} = \frac{4eR^2}{J}\Phi^\alpha\left[\hat\sigma^y_{\alpha\beta}\hat{\boldsymbol{p}} - 2e\boldsymbol{A}\delta_{\alpha\beta}\right]\Phi^\beta. \quad (16)$$

This relation holds on the classical field theory level, and it is translated to an operator identity of the corresponding quantum theory.

III. GAUSSIAN FLUCTUATIONS AND PARACONDUCTIVITY

In this section we consider the fluctuation propagator of the order parameter $L(\omega,\boldsymbol{q})$ in the simplest Gaussian approximation, and calculate the corresponding fluctuation contribution to electric conductivity.

A. Order-parameter propagator

On the Gaussian level, the order-parameter Green function $\check L$ is given by the Dyson series shown on Fig. 2, with analytic expression given by

$$\check L^{-1} = (\check L^{(0)})^{-1} - \check S, \quad (17)$$

$$S^{\alpha\beta}_{\mu\nu}(\omega) = \frac{i}{2}\int\frac{d\Omega}{2\pi}\operatorname{Tr}[\check\Gamma_\mu\hat\sigma^\alpha\hat G(\Omega+\omega)\check\Gamma_\nu\hat\sigma^\beta\hat G(\Omega)]. \quad (18)$$

The expression for the self-energy part coincides with the unperturbed spin-spin–correlation function $S_i^{\alpha\beta}(t-t') = i\langle\hat\sigma_i^\alpha(t)\hat\sigma_i^\beta(t')\rangle$. Note that $\hat S$ is a diagonal in real-space matrix, which depends on the onsite random energy ε_i. Since we are interested in $\langle L\rangle_\varepsilon$, we need to average the whole Dyson series (Fig. 2). We employ an approximation of large radius R which guarantees that propagator L changes considerably on a long spatial scale which includes many individual "spins" S_i; thus, we can build a kind of "impurity diagram technique" with regard to random local fields ε_i.

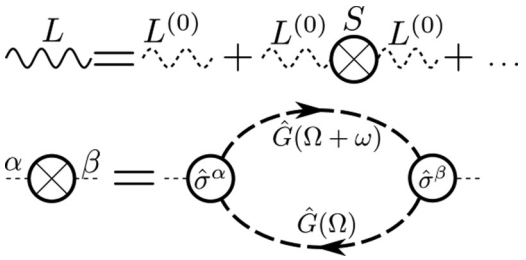

FIG. 2. Upper figure: Dyson series for the order-parameter Green function L given by Eq. (17); dashed wavy line corresponds to $\hat{L}^{(0)} = \hat{J}/2$. The crossed circle, shown in the lower figure, is spin-spin–correlation function $\hat{S}$ given by (18) acts as the "polarization operator" for the order-parameter propagator. The crossed circle indicates that it is a diagonal operator in real space (but it still has nontrivial time structure). Spin-space indices $\alpha,\beta \in \{x,y,z\}$; vertices have also Keldysh structure $\check{\Gamma}_\mu$, $\mu \in \{cl,q\}$. Dashed lines correspond to the semionic Green functions given by (13).

The Dyson equation for the average propagator $\langle\check{L}\rangle$ reads as

$$\langle\check{L}\rangle_\varepsilon^{-1} = (\check{L}^{(0)})^{-1} - \check{\Pi}. \tag{19}$$

To the leading order in large R we can average all the $\check{S}_i$ independently and put $\check{\Pi} \approx \langle\check{S}\rangle_\varepsilon$. In Sec. V we will take into account additional terms beyond this simplest approximation.

We now proceed with the calculation of the self-energy (18). The Keldysh space can be traced out immediately; the retarded ($\mu = q$, $\nu = cl$) component reads as follows:

$$S_R^{\alpha\beta}(\omega) = \frac{i}{2}\int\frac{d\Omega}{2\pi}\,\mathrm{Tr}\,(\hat{\sigma}^\alpha\hat{G}_R(\Omega+\omega)\hat{\sigma}^\beta\hat{G}_K(\Omega) + \hat{\sigma}^\alpha\hat{G}_K(\Omega+\omega)\hat{\sigma}^\beta\hat{G}_A(\Omega)). \tag{20}$$

We perform all the calculations by keeping γ finite, as we will refer to them later in Sec. IV B; however, within Gaussian approximation for fluctuations the limit $\gamma \to 0$ is sufficient. The terms arising after substitution of semionic bare propagators given by Eq. (13) can be divided onto two groups. The first group corresponds to semions residing on the same branch, $\propto G^\uparrow G^\uparrow$ or $\propto G^\downarrow G^\downarrow$. It appears to vanish in the limit $\gamma \to 0$, while for finite γ it is odd in $\varepsilon \mapsto -\varepsilon$ and thus vanishes upon further averaging over ε. The second group, where semions reside in different branches, can itself be naturally divided into diagonal and off-diagonal in spin-space parts. Introducing the unit vector in the z direction $\boldsymbol{n} = (0,0,1)$, and performing the energy integration, we obtain following results:

$$S_R^{\alpha\beta}(\omega) = (\delta^{\alpha\beta} - n^\alpha n^\beta)S_R^{(\mathrm{diag})}(\omega) + i\epsilon^{\alpha\beta\mu}n^\mu S_R^{(\mathrm{off})}(\omega), \tag{21}$$

where in the limit $\gamma \ll T,\varepsilon$ we find

$$S_R^{(\mathrm{diag})}(\omega) \approx \frac{\mathfrak{f}(\varepsilon)\varepsilon}{\varepsilon^2 - (\omega/2 + i\gamma)^2}, \tag{22}$$

$$S_R^{(\mathrm{off})}(\omega) \approx \frac{\mathfrak{f}(\varepsilon)\omega/2}{\varepsilon^2 - (\omega/2 + i\gamma)^2}, \tag{23}$$

and $\mathfrak{f}(\varepsilon)$ is given by Eq. (15). In the limit $\gamma \to +0$, these correlation functions describe trivial dynamics of a single-spin precession in a constant magnetic field $\varepsilon\boldsymbol{n}$.

The next step is to perform averaging over ε to calculate $\Pi_R(\omega) \approx \langle S_R(\omega)\rangle_\varepsilon$. The off-diagonal part is odd in $\varepsilon \mapsto -\varepsilon$ even at finite γ and vanishes upon averaging, thus, the only nontrivial contribution is due to $S_R^{(\mathrm{diag})}(\omega)$. In the limit $\omega \ll T$, it is natural to consider real and imaginary parts of the correlation function independently. The real part is static, it determines the critical temperature of the transition, while the imaginary part is ω dependent and describes purely dissipative dynamics of the order-parameter fluctuations:

$$\left\langle \mathrm{Re}\, S_R^{(\mathrm{diag})}(\omega)\right\rangle \approx \left\langle\frac{\mathfrak{f}(\varepsilon)}{\varepsilon}\right\rangle_\varepsilon = \frac{1}{W}\ln\frac{4e^\gamma W}{\pi T}, \tag{24}$$

$$\left\langle \mathrm{Im}\, S_R^{(\mathrm{diag})}(\omega)\right\rangle = \pi\nu_0\mathfrak{f}\left(\frac{\omega}{2}\right) \approx \frac{\pi\omega}{4WT}. \tag{25}$$

Note that the major contribution to the static part comes from logarithmically broad energy range between $T \ll \varepsilon \ll W$, while the imaginary part is given by $\varepsilon \sim \omega$ as it describes real resonant spin-flip processes which lead to the dissipation of the order-parameter fluctuations. The presence of a linear in ω term is thus a direct consequence of the nonzero single-spin density of states $\nu_0 = P(\varepsilon \ll T)$.

The above calculation leads to the following form of the order-parameter propagator:

$$L_R(\omega,\boldsymbol{q}) = \frac{1/2\nu_0}{\epsilon + q^2\xi_0^2 - i\omega\tau}, \tag{26}$$

with

$$\epsilon = \ln\frac{T}{T_c} \approx \frac{T - T_c}{T_c} \ll 1, \quad \xi_0 = \frac{R}{\sqrt{g}}, \quad \tau = \frac{\pi}{4T}, \tag{27}$$

and T_c given by the same expression as given above (7). The dimensionless parameter ϵ describes the distance to the superconducting transition, ξ_0 corresponds to the "zero-temperature" coherence length, and τ^{-1} defines the decay rate of the collective mode far from T_c. At small ϵ, coherence length and relaxation time diverge as $\xi(\epsilon) = \xi_0/\sqrt{\epsilon}$ and τ/ϵ, correspondingly.

We should emphasize that the form of the propagator (26) is independent of the exact shape of the distribution function provided it has nonzero DOS $\nu_0 = P(\varepsilon = 0)$ and does not change significantly at $\varepsilon \lesssim \omega$. The only parameter sensitive to the exact shape is T_c.

This form of the propagator is reminiscent of the ordinary time-dependent Ginzburg-Landau (TDGL) [23] theory describing the dynamics of the order parameter in the metals close to the superconducting transition. The difference is that in our theory ξ_0 does not scale with T_c as it does in disordered metals, where $\xi_0 \sim \sqrt{D/T_c}$; another important difference is that the parameter τ we found is twice larger compared to the value known for disordered metals, where $\tau = \pi/8T$.

B. Fluctuational conductivity

We found in the preceding section that dynamics of our order parameter appears to be similar to the usual TDGL. Paraconductivity in superconductors above T_c was calculated a long time ago by Aslamazov and Larkin [17], while its calculation using TDGL formalism can be found in Ref. [23].

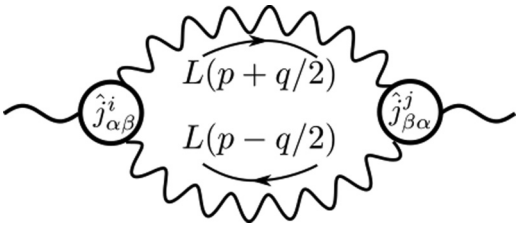

FIG. 3. Diagrammatic representation of Q kernel given by Eq. (29). Wavy lines correspond to the order-parameter Green functions $L(\omega,\boldsymbol{q})$, and current vertices are $\hat{j}^i_{\alpha\beta} = \frac{4R^2}{J}\hat{\sigma^y}_{\alpha\beta}(-i\nabla^i)$ [see Eq. (16)].

In this section we briefly recapitulate the calculation and discuss the obtained results.

In order to obtain the expression for the electric conductivity of the system, one can apply the Kubo formula

$$\sigma^{ij}(\omega,\boldsymbol{q}) = i\,\frac{Q^{ij}_R(\omega,\boldsymbol{q}) - Q^{ij}_R(0,\boldsymbol{q})}{\omega}, \tag{28}$$

where current-current correlation function in real space-time reads as

$$Q^{ij}_{\mu\nu}(\boldsymbol{r}-\boldsymbol{r}',t-t') = -i\left\langle j^i_\mu(\boldsymbol{r},t)\,j^j_\nu(\boldsymbol{r}',t')\right\rangle, \tag{29}$$

and Eq. (28) contains its Fourier transform to $(\boldsymbol{q},\omega)$ representation.

Within the Gaussian approximation over fluctuations, the only diagram contributing to the Q kernel is given by Fig. 3, and the corresponding expression yields [here $p_\pm = p \pm \frac{q}{2}$, $p = (\Omega,\boldsymbol{p})$, and $q = (\omega,\boldsymbol{q})$]

$$Q^{ij}_R(\omega,\boldsymbol{q}) = 32i\nu_0^2\xi_0^2e^2\int\frac{d\Omega}{2\pi}\frac{d^d\boldsymbol{p}}{(2\pi)^d}p^i\,p^j \times [L_R(p_+)L_K(p_-) + L_K(p_+)L_A(p_-)]. \tag{30}$$

Note here that in the static limit $\omega\to 0$, the expression for the uniform ($q=0$) Aslamazov-Larkin conductivity is diagonal and reads as $\sigma_{\rm AL} = i\,\partial Q_R/\partial\omega$, which can be further simplified:

$$\sigma_{\rm AL} = \frac{16}{d}\nu_0^2\xi_0^4e^2\int\frac{d\Omega}{2\pi}\frac{d^d\boldsymbol{p}}{(2\pi)^d}\boldsymbol{p}^2\mathfrak{B}'(\Omega)(\Delta L(\Omega,\boldsymbol{p}))^2. \tag{31}$$

Now, we substitute Eq. (26) for the propagator $L(\omega,\boldsymbol{q})$, perform integration over energy using residues, and switch to integration over dimensionless momentum $P = p\xi_0/\sqrt{\epsilon}$ to arrive at

$$\sigma_{\rm AL} = \frac{e^2}{\xi_0^{d-2}\epsilon^{2-d/2}}\frac{8}{d}T\tau\int\frac{d^d\boldsymbol{P}}{(2\pi)^d}\frac{P^2}{(1+P^2)^3} \equiv \frac{e^2 s_d}{\xi_0^{d-2}\epsilon^{2-d/2}}, \tag{32}$$

where $s_2 = \frac{1}{8}$ and $s_3 = \frac{1}{16}$. Finally, we find paraconductivity in the form

$$\sigma_{\rm AL} = \frac{e^2}{\hbar}\times\begin{cases}1/8\epsilon, & \text{(2D)}\\ 1/16\xi_0\sqrt{\epsilon}, & \text{(3D)}\end{cases} \tag{33}$$

(where we have restored $\hbar$ by dimensionality). This result appears to be twice larger compared to the ordinary Aslamazov-Larkin result [17]. The discrepancy can be traced back to the fact that τ is twice larger compared to the ordinary metals, which we have briefly mentioned above. While in ordinary superconductors the AL paraconductivity provides a relatively small correction to the standard Drude conductivity σ_D, in our system with a large pseudogap, paraconductivity $\sigma_{\rm AL}$ may occur to be the dominant contribution: the only alternative conduction channel is due to individual electrons hopping between localized states, whose contribution is suppressed additionally due to $T_c \ll \Delta_P$ condition. For the same reason, one should not worry about other fluctuational corrections to conductivity (of the Maki-Thompson and DOS types) which are known to exist [23] in usual disordered superconductors. Indeed, usual types of corrections are related with modification of single-electron conductivity due to pairing correlations, while in our case single-particle transport is suppressed due to large pseudogap.

Below we will study different kinds of corrections to the Gaussian approximation we used, and show that Eq. (33) provides a very good approximation if $\epsilon \geqslant \epsilon_1$ [see Eqs. (38) and (39)]. Then, we analyze corrections that appear at smaller values of ϵ.

IV. LOCAL NOISE EFFECT

Non-Gaussian effects due to interaction between fluctuating collective modes are generally known to become important for thermodynamics quantities in the close proximity of the critical point at $\epsilon \leqslant {\rm Gi}$, where Ginzburg number ${\rm Gi}\sim Z^{-2/(4-d)}$. However, it was noticed in Ref. [19] that for dynamics quantities (in particular, for paraconductivity) interaction corrections may become large in a parametrically broader range of reduced temperature ϵ. In this section we show that a similar phenomenon comes about in our model as well. Namely, we find a rather special type of interaction corrections that affect the dependence of the relaxation time $\tau_{\rm GL}$ on ϵ, which become relevant already at $\epsilon \leqslant \epsilon_1 \sim {\rm Gi}^{1/d}$, whereas all static quantities are still well described within the Gaussian approximation.

Specific kind of interaction corrections relevant at $\epsilon \leqslant \epsilon_1$ can be understood as a result of local "back-action" of the order-parameter (superconducting) fluctuations upon dynamics of individual "pseudospins" S_i. Indeed, Keldysh action (11) describes its dynamics under the fluctuating local "magnetic field" $(\Phi^x_i(t),\Phi^y_i(t),\varepsilon_i)$. Since local correlation functions of the field $\boldsymbol{\Phi}_i(t)$ coincide with the propagator $L(\omega,\boldsymbol{r},\boldsymbol{r}')$ calculated at $\boldsymbol{r}=\boldsymbol{r}'=\boldsymbol{r}_i$, the action (11) together with Dyson equation (17) constitute a closed set of self-consistent equations. Solution of these equations would involve (i) finding dynamical correlation functions of a spin S_i under the action of dynamic magnetic field with a given correlation function of the local "noise function" $C_i(t-t') = \langle\Phi^\alpha_i(t)\Phi^\beta_i(t')\rangle$; (ii) calculation of the propagator $L(\omega,\boldsymbol{r},\boldsymbol{r}')$ via Dyson equation; (iii) self-consistent determination of the local noise function for each site i. In general, the above scheme contains a macroscopic number of variables and thus it is very complicated. The problem can be grossly simplified if site-i-dependent noise function can be approximated by a single universal function: $C_i(t-t')\to C(t-t')$. In Sec. V we will see that such an approximation is indeed valid in the range ${\rm Gi}\ll\epsilon\leqslant\epsilon_1$. Currently, we take it for granted and study the effect of such a transverse noise

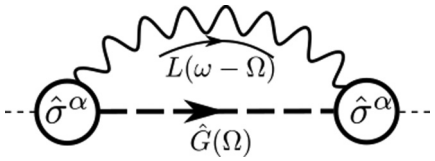

FIG. 4. Semionic self-energy correction $\hat{\Sigma}(\omega)$ due to its interaction with the order parameter, which describes the "spin noise" effect.

upon local spin-spin dynamics, order-parameter dynamics, and, eventually, upon paraconductivity.

The key characteristic of the noise is provided by the propagator at the coinciding points $L(\omega, \boldsymbol{r} = \boldsymbol{r}')$. This quantity itself is ultraviolet divergent (with momentum integration should be cut off at $\Lambda \sim R^{-1}$), but relevant ω- and ϵ-dependent parts can be separated and are determined by the infrared behavior:

$$L_R(\omega) \approx \frac{1}{8\pi\nu_0\xi_0^d}\begin{cases}\ln(\Lambda^2\xi_0^2) - \ln(\epsilon - i\omega\tau), & \text{(2D)}\\ \Lambda\xi_0 - \sqrt{\epsilon - i\omega\tau}, & \text{(3D)}.\end{cases} \tag{34}$$

The "local noise" described by this propagator is small provided ξ_0 is large enough.

A. Spin relaxation and renormalization

The effect of the "noise" caused by the order-parameter fluctuations on the spin-correlation function can be studied perturbatively using the Keldysh action (11). There are, in general, two types of such corrections: to a semionic propagator and to a vertex part, and we start from the first one.

The simplest diagram for the semionic propagator correction is shown on Fig. 4. Below we will focus only on the "$\downarrow$" semionic branch, as the expressions for "$\uparrow$" can be obtained simply by replacing $\varepsilon \to -\varepsilon$. The corresponding analytic expression for the retarded component of the self-energy reads as

$$\Sigma_R^{\downarrow}(\omega,\varepsilon) = -\frac{i}{2}\int\frac{d\Omega}{2\pi}[G_R^{\uparrow}(\Omega)L_K(\omega-\Omega) + G_K^{\uparrow}(\omega-\Omega)L_R(\Omega)]. \tag{35}$$

For $\omega \ll T$ one can neglect the second term proportional to semionic "distribution function" $\mathfrak{F}(\omega)$ because the bosonic one is singular $\mathfrak{B}(\omega) \approx 2T/\omega$. Under this assumption, the self-energy part depends only on the simple combination of ω and ε, namely, $\Sigma_R^{\downarrow,\uparrow}(\omega,\varepsilon) \equiv \Sigma_R(\Omega = \omega \pm \varepsilon)$ with

$$\Sigma_R(\Omega) = \frac{T}{8\pi\nu_0\xi_0^d\Omega}\begin{cases}\ln\frac{\epsilon - i\Omega\tau}{\epsilon}, & \text{(2D)}\\ \sqrt{\epsilon - i\Omega\tau} - \sqrt{\epsilon}, & \text{(3D)}.\end{cases} \tag{36}$$

Although semions do not correspond to real quasiparticles in the system, their properties nevertheless describe the physical spin-correlation function. Namely, $\mathrm{Im}\,\Sigma_R$ corresponds to the real processes of spin relaxation, and $\mathrm{Re}\,\Sigma_R$ describes renormalization of the spectrum. In the lowest order of perturbation theory, these two effects can be studied separately, and we start with the spin-relaxation processes.

The spin-flip rate γ, which enters the semionic Green function exactly as infinitesimal γ did in Eq. (13), is defined by the imaginary part of Σ_R taken on the "mass shell" $\omega = \varepsilon \Rightarrow \Omega = 2\varepsilon$:

$$\gamma(\varepsilon) \approx \frac{T}{8\pi\nu_0\xi_0^d}\frac{1}{\varepsilon}\cdot\begin{cases}\arctan\frac{2\varepsilon\tau}{\epsilon}, & \text{(2D)}\\ \mathrm{Im}\sqrt{\epsilon + 2i\varepsilon\tau} & \text{(3D)}.\end{cases} \tag{37}$$

This rate was obtained on the perturbative level, and is valid only provided the rate is small compared to the spin-coherent precession frequency $\gamma(\varepsilon) \ll \varepsilon$. This criterion clearly cannot be satisfied for all ε as $\gamma(\varepsilon \to 0)$ approaches constant value. A new energy scale ω_c emerges, that separates spins with mainly dissipative dynamics ($\varepsilon \ll \omega_c$) from spins with coherent dynamics ($\varepsilon \gg \omega_c$). This effect can affect paraconductivity if the energy scale ω_c is large enough, namely, if $\omega_c \gg \epsilon T$ (note that ω_c itself can, in principle, depend on ϵ). The above criterion can be reformulated as a criterion for proximity to the transition $\epsilon \ll \epsilon_1$ with

$$\epsilon_1 = \rho^{1/2}, \qquad \rho = \frac{1}{16\nu_0\xi_0^2 T} = \frac{gW}{8R_0^2T_c}, \qquad \text{(2D)} \tag{38}$$

$$\epsilon_1 = \rho^{2/3}, \quad \rho = \frac{1}{16\sqrt{\pi}\nu_0\xi_0^3 T} = \frac{g^{3/2}W}{8\sqrt{\pi}R_0^3T_c}, \quad \text{(3D)}. \tag{39}$$

The form of the expression for ω_c depends on the reduced temperature ϵ:

$$\epsilon \gg \epsilon_1 : \omega_c = \begin{cases}T\rho/\epsilon, & \text{(2D)}\\ T\rho\sqrt{\pi/4\epsilon}, & \text{(3D)}\end{cases} \tag{40}$$

$$\epsilon \ll \epsilon_1 : \omega_c = \begin{cases}T\rho^{1/2}, & \text{(2D)}\\ T\rho^{2/3}, & \text{(3D)}.\end{cases} \tag{41}$$

For the whole analysis to be consistent, we need the condition $\rho \ll 1$ to be fulfilled. Parameter ρ is inversely proportional to the coordination number $\rho \sim 1/Z$.

The real part of the self-energy $\mathrm{Re}\,\Sigma_R$ renormalizes the spectral weight of the spin-correlation function $\mathrm{Im}\,S_R$ in the following manner:

$$\mathrm{Im}\,S_R^{(\mathrm{diag})}(\omega) = \frac{1}{4}\int\frac{d\Omega}{2\pi}[\Delta G^{\downarrow}(\Omega+\omega)\Delta G^{\uparrow}(\Omega) + \{\uparrow \leftrightarrow \downarrow\}] \times [\mathfrak{F}(\Omega) - \mathfrak{F}(\Omega+\omega)]. \tag{42}$$

Since we are studying two effects from $\mathrm{Im}\,\Sigma_R$ and $\mathrm{Re}\,\Sigma_R$ separately, it is sufficient to substitute $\Delta G^{\uparrow,\downarrow}(\omega) = -2\pi i\delta[\omega \pm \varepsilon - \mathrm{Re}\,\Sigma_R(\omega \mp \varepsilon)]$; at low frequencies we arrive at

$$\mathrm{Im}\,S_R^{(\mathrm{diag})}(\omega) = \frac{\pi\omega}{2T}\big[[1 - \mathrm{Re}\,\Sigma_R'(2\varepsilon)]^{-1}\delta[2\varepsilon - \omega + \mathrm{Re}\,\Sigma_R(2\varepsilon) - \mathrm{Re}\,\Sigma_R(\omega)] + \{\varepsilon \mapsto -\varepsilon\}\big]. \tag{43}$$

This spectral weight affects relaxation time of the order parameter τ via the relation

$$\omega\tau = \frac{1}{2\nu_0}\big\langle \mathrm{Im}\,S_R^{(\mathrm{diag})}(\omega)\big\rangle_{\varepsilon}. \tag{44}$$

However, evaluation of Eq. (44) shows that the Gaussian value for the important parameter $T\tau = \pi/4$ remains unchanged. We conclude that on the lowest order of perturbation theory, the effect coming from $\mathrm{Re}\,\Sigma_R$ does not affect the order-parameter

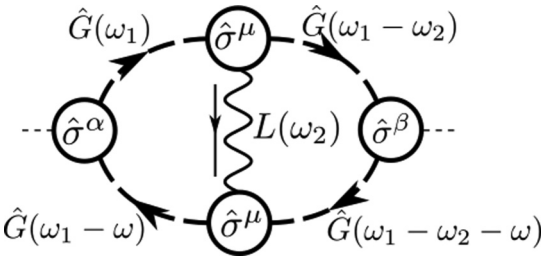

FIG. 5. Vertex correction to the order-parameter self-energy (Fig. 2) connecting upper and lower semionic lines. This diagram vanishes due to its spin structure.

dynamics (and thus paraconductivity), and it is sufficient to focus on the spin-relaxation processes only.

Finally, let us focus on the vertex-part corrections to the spin-correlation function shown in Fig. 5; the corresponding analytic expression reads as

$$\delta S^{\alpha\beta}_{\mu\nu}(\omega) = -\frac{1}{4}\int \frac{d\omega_1}{2\pi}\frac{d\omega_2}{2\pi} L^{\gamma\delta}_{\lambda\rho}(\omega_2)\,\mathrm{Tr}\,(\check{\Gamma}_\mu \hat{\sigma}^\alpha \hat{G}(\omega_1)\hat{\sigma}^\gamma \check{\Gamma}_\lambda \times \hat{G}(\omega_1-\omega_2)\check{\Gamma}_\nu \hat{\sigma}^\beta \hat{G}(\omega_1-\omega_2-\omega) \times \hat{\sigma}^\delta \check{\Gamma}_\rho \hat{G}(\omega_1-\omega)). \quad (45)$$

After working out the spin structure, one can see that two nontrivial contributions are proportional to $\mathrm{Tr}(\hat{\sigma}^\alpha \hat{\mathbb{P}}^\uparrow \hat{\sigma}^\mu \hat{\mathbb{P}}^\downarrow \hat{\sigma}^\beta \hat{\mathbb{P}}^\uparrow \hat{\sigma}^\mu \hat{\mathbb{P}}^\downarrow)$ (and the same with $\uparrow \leftrightarrow \downarrow$); and after summation over $\mu = x, y$, these contributions exactly vanish. We conclude that lowest-order nontrivial correction comes only from dressing semionic Green function in the loop, as it is shown in Fig. 4.

B. Correction to the order-parameter propagator

The semionic renormalization discussed above affects the spin-correlation function, which enters the Dyson equation for the order parameter. The prime effect is upon the dissipative part of the order-parameter propagator $L(\omega,\boldsymbol{q})$, which is determined by the spectral weight of the spin-correlation function [see Eq. (44)]. The major contribution to the above average over local energies ε comes from $\varepsilon \sim \omega \ll T$, thus, the factor linear in ω comes just from the expansion of the Fermi distribution function $\mathfrak{f}(\omega) \approx \beta\omega$. This allows us to write the following formula for the important dimensionless parameter $T\tau$, which now can depend on frequency ω (we remind that paraconductivity is proportional to it, and on the Gaussian level this parameter was $\pi/4$):

$$T\tau(\omega) = -\frac{1}{4\nu_0}\int \frac{d\Omega}{2\pi}\langle \Delta G^\downarrow(\Omega+\omega)\Delta G^\uparrow(\Omega)\rangle_\varepsilon. \quad (46)$$

In the previous section, we have shown that real part of semionic self-energy $\mathrm{Re}\,\Sigma_R$ does not affect the product $T\tau$, while $\mathrm{Im}\,\Sigma_R$ can be accounted for by the substitution of the propagators in the form (13) with nonzero γ, given by (37):

$$T\tau(\omega) = \frac{1}{4}\int \frac{d\varepsilon\,\gamma(\varepsilon)}{\gamma^2(\varepsilon)+(\varepsilon-\omega/2)^2}. \quad (47)$$

Integration can be performed numerically (plots are shown on Fig. 6). Striking feature of all the curves is that they exhibit

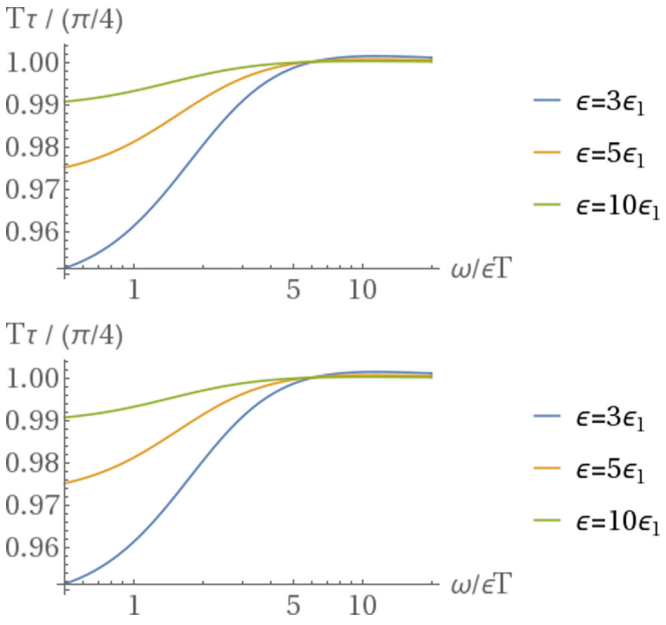

FIG. 6. Frequency dependence of $T\tau(\omega)$ for 2D (upper) and 3D (lower) at $\epsilon = 3\epsilon_1$ (blue), $\epsilon = 5\epsilon_1$ (orange), and $\epsilon = 10\epsilon_1$ (green) as given by Eq. (47).

nonmonotonous behavior. This analysis is consistent provided $\omega \geqslant \omega_c$, where the deviation of $T\tau$ from $\pi/4$ is small.

At low frequencies $\omega \lesssim \omega_c$ the kinetic term in the propagator $L(\omega,\boldsymbol{q})$ is governed by the contribution coming from the spins with local fields $\varepsilon \lesssim \omega_c$, which obey nearly dissipative dynamics, which is difficult for analytical study. However, it is still possible to bring up some qualitative arguments that show that the product $T\tau$ retains the same order of magnitude and can be modified by some numerical factor ~ 1 only. First, we note that at $\varepsilon \ll \omega_c$ coherent contribution to spin dynamics is negligible (formally, we set here $\varepsilon = 0$) and the only energy scale that governs dynamics of these spins is given by ω_c. Symmetrized spin-spin correlation $C(t-t') = \langle\{S^+(t), S^-(t')\}\rangle = \varphi(\omega_c|t-t'|)$ where function $\varphi(z)$ decays fast at $z \gg 1$, while $\varphi(0) = 1$. After transformation to the frequency domain, we find that the Keldysh component of the spin-correlation function is $S_K^{(\mathrm{diag})}(\omega) \simeq \frac{1}{\omega_c}\tilde{\varphi}(\frac{\omega}{\omega_c})$, where $\tilde{\varphi}(z)$ is some even function. Using now the fluctuation-dissipation relation, one finds that $\mathrm{Im}\,S_R^{(\mathrm{diag})}(\omega) \simeq -\frac{\omega}{\omega_c T}\tilde{\varphi}(\frac{\omega}{\omega_c})$. This form can be used now together with Eq. (44), in order to estimate the product $T\tau$. Fraction of spins with small local energies $\varepsilon_i \leqslant \omega_c$ is of the order of $\sim\omega_c/W$. Multiplying it with $\mathrm{Im}\,S_R^{(\mathrm{diag})}(\omega)$ and using Eq. (44), we find that $T\tau \sim \tilde{\varphi}(0) \sim 1$.

This qualitative argument shows that the $T\tau(\omega \ll \omega_c)$ is still a constant of the order of unity, which, however, may differ from the $\pi/4$.

C. Effect on the paraconductivity

Let us now study the implication of the non-Gaussian effect discussed above upon the paraconductivity. We need to consider the corrections to the Q kernel given by Fig. 3. In the leading order one should consider the same diagram, but

with dressed order-parameter Green functions, which we have studied in the previous section.

As it can be seen from the calculation in Sec. III B, the main contribution to the paraconductivity comes from the order-parameter fluctuations with energies $\omega\tau \sim \epsilon$ and momenta $p\xi_0 \sim \sqrt{\epsilon}$. In the previous section we have shown that the back effect coming from the dynamics of "noisy spins" changes the constant $T\tau(\omega)$ at frequencies $\omega \lesssim \omega_c$ only. Thus, we conclude that this renormalization is negligible provided $\omega_c \ll \epsilon T = |T - T_c|$, which, in turn, leads to the applicability criterion for Eq. (33) in a form $\epsilon \geqslant \epsilon_1$ with ϵ_1 given by Eqs. (38) and (39).

At smaller ϵ, the contribution of spins whose dynamics is strongly affected by the noise, becomes dominant. However, as we saw in the previous subsection, this effect can hardly change the kinetic coefficient τ more substantially than by some factor of order unity; therefore, we expect Aslamazov-Larkin–type paraconductivity [Eq. (33)] to be valid qualitatively even at smaller ϵ, down to $\epsilon \geqslant \rho^{2/(4-d)}$. Another type of correction that comes into play at still lower ϵ will be considered in the next section.

V. OTHER TYPES OF FLUCTUATIONAL CORRECTIONS

In the previous section a special kind of a fluctuational correction was demonstrated, which becomes relevant for kinetic properties of our system in a relatively broad range of reduced temperatures $\epsilon \leqslant \epsilon_1$, where $\epsilon_1 \sim \rho^{1/2}$ in 2D and $\epsilon_1 \sim \rho^{2/3}$ in 3D. On the other hand, a standard Ginzburg criterion for the width of the fluctuation-dominated region near second-order phase transition reads as $\epsilon \leqslant \epsilon_2 \equiv \mathrm{Gi} \sim Z^{-\frac{2}{4-d}}$, where $Z \sim 1/\rho$ is an effective number of "interacting neighbors" [see Eqs. (38) and (39)]. Thus, we conclude that $\epsilon_2 \sim \epsilon_1^d \ll \epsilon_1$ for $d = 2,3$.

Below we will consider some additional corrections to the Gaussian approximation of Sec. III, which are specific to the presence of strong disorder in our model; we will show that these effects also become relevant at $\epsilon \leqslant \epsilon_2$ only. Namely, we concentrate on the corrections to the approximation $\check{\Pi} = \langle \check{S} \rangle_\varepsilon$ for the self-energy of the order-parameter propagator $L(\omega,\boldsymbol{q})$, as defined by the Dyson equation (19).

In the calculation shown in Sec. III A we have studied the order-parameter propagator averaged over the disorder by means of the Dyson equation (19), where in the leading approximation we used the self-energy $\check{\Pi} = \langle \check{S} \rangle_\varepsilon$. The same approximation was employed in the calculation of all other quantities we have studied, including paraconductivity itself. In this section we will study the deviations from the results of this approximation, using the semion diagram technique.

A. Corrections to $L(\omega,q)$

Locator expansion for the propagator $L(\omega,\boldsymbol{q})$ averaged over distribution of $\{\varepsilon_i\}$ contains terms of the form $\check{L}^{(0)}\check{S}\check{L}^{(0)}\check{S}\ldots\check{S}\check{L}^{(0)}$. Previously, we proceeded with separate averaging of each $\check{S}$ term in this expansion. The first correction to this approximation contains simultaneous averaging of two locators $\check{S}$, as shown in Fig. 7; the corresponding analytical expression is $\langle S_R^{\alpha\mu}(\omega_1) S_R^{\nu\beta}(\omega_2)\rangle_\varepsilon$. We present calculations of such an object in Appendix C, making use of Eqs. (21)–(23). For our purpose it is sufficient to consider here the limit of

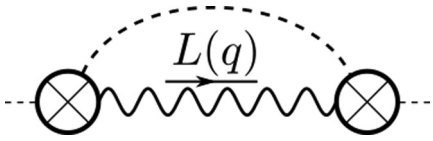

FIG. 7. Correction to the averaged over disorder order-parameter self-energy $\check{\Pi} - \langle \check{S} \rangle_\varepsilon$. Dashed "impurity" line corresponds to simultaneous averaging of two spin-correlation functions $\check{S}$ over ε

$\omega_{1,2} \to 0$, to obtain

$$\left\langle \left(S_R^{(\mathrm{diag})}(0)\right)^2 \right\rangle_\varepsilon \approx \frac{14\zeta(3)}{\pi^2 WT}. \tag{48}$$

The structure of the correction shown in Fig. 7 appears to be diagonal in the (α,β) space, $\delta\Pi_R^{\alpha\beta}(\omega) = (\delta^{\alpha\beta} - n^\alpha n^\beta)\delta\Pi_R(\omega)$, and the whole correction to the self-energy is given by

$$\delta\Pi_R(\omega) = L_R(\omega)\left\langle \left(S_R^{(\mathrm{diag})}(0)\right)^2 \right\rangle. \tag{49}$$

The static ($\omega = 0$) contribution to $\delta\Pi_R(\omega)$ corresponds to the renormalization of T_c, which was already studied in Appendix A [see Eq. (A12) and comments below]. The frequency-dependent part at $\omega\tau \ll \epsilon$ contains a singularity at small ϵ:

$$\delta\Pi_R(\omega) - \delta\Pi_R(0) \approx -\frac{i\omega\tau}{4\pi T\xi_0^d} \times \begin{cases} \frac{14\zeta(3)}{\pi^2\epsilon}, & (2\mathrm{D}) \\ \frac{7\zeta(3)}{\pi^2\sqrt{\epsilon}}, & (3\mathrm{D}) \end{cases} \tag{50}$$

which should be compared with the bare ω-dependent term in $L^{-1}(\omega,\boldsymbol{q})$ [see Eq. (26)]. Then, we find that the correction (50) is small provided

$$\begin{cases} \epsilon \gg \frac{W}{T\xi_0^2} \sim \rho, & (2\mathrm{D}) \\ \epsilon \gg \left(\frac{W}{T\xi_0^3}\right)^2 \sim \rho^2, & (3\mathrm{D}) \end{cases} \tag{51}$$

which coincides with the usual Ginzburg criterion discussed in the beginning of this section.

B. Spatial fluctuations of the conductivity

It was assumed implicitly during the calculation of paraconductivity in Sec. III B (and further discussion in Sec. IV C) that conductivity is uniform through the system and thus can be characterized as the kernel $\sigma(\boldsymbol{r} - \boldsymbol{r}')$ in the linear relation between current density and electric field $\boldsymbol{j}(\boldsymbol{r}) = \int \sigma(\boldsymbol{r} - \boldsymbol{r}')\boldsymbol{E}(\boldsymbol{r}')d^3r'$. In the disordered medium, conductivity contains spatial fluctuations, so that the kernel becomes a function of two coordinates separately $\sigma(\boldsymbol{r} - \boldsymbol{r}') \to \sigma(\boldsymbol{r},\boldsymbol{r}')$. In order to satisfy current conservation law $\partial_\alpha j_\alpha = 0$, with the current given by $j_\alpha(\boldsymbol{r}) = \int \sigma(\boldsymbol{r},\boldsymbol{r}')E_\alpha(\boldsymbol{r}')d\boldsymbol{r}'$, the local electric field E_α must fluctuate in space:

$$\delta E_\alpha(\boldsymbol{r}) = -\frac{1}{d\overline{\sigma}}\overline{E}_\alpha \int \delta\sigma(\boldsymbol{r},\boldsymbol{r}')d\boldsymbol{r}'. \tag{52}$$

It results [24] in the additional contribution to the average conductivity of the form

$$\frac{\delta\sigma}{\bar{\sigma}} = -\frac{1}{d}K(\mathbf{r} = 0), \tag{53}$$

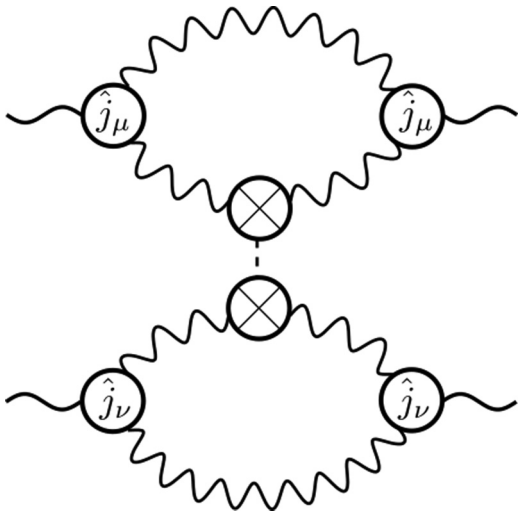

FIG. 8. Lowest-order diagram representing the fluctuations of the conductivity $K(\boldsymbol{r}-\boldsymbol{r}')$.

where correlation function $K(\boldsymbol{r}-\boldsymbol{r}')$ is defined as follows:

$$K(\boldsymbol{r}-\boldsymbol{r}') = \frac{1}{\bar{\sigma}^2}\int d\boldsymbol{x}\, d\boldsymbol{y}\langle\delta\sigma(\boldsymbol{r},\boldsymbol{x})\delta\sigma(\boldsymbol{r}',\boldsymbol{y})\rangle. \tag{54}$$

Below we will calculate this correlation function $K(\boldsymbol{r}-\boldsymbol{r}')$. The diagram of the lowest order is shown in Fig. 8. This diagram consists of two parts: two independent loop integrals, which are similar to the Q kernel given by Eq. (30) and which we denote as $\mathcal{R}^{ij}(\omega,\boldsymbol{q})$, and an "impurity line," which to the leading order can be taken in the static limit $\langle(S_R^{(\mathrm{diag})}(0))^2\rangle$. Since one can put an "impurity" either on upper or lower Green function, which corresponds to replacement $q \mapsto -q$ in the expression for $\mathcal{R}^{\mu\nu}(\omega,\boldsymbol{q})$, there are, in total, four terms in the expression for the conductivity fluctuations:

$$K(\boldsymbol{q}) = \left\langle\left(S_R^{(\mathrm{diag})}(0)\right)^2\right\rangle\left[\frac{i\partial_\omega[\mathcal{R}^{ii}(\omega,\boldsymbol{q})+\mathcal{R}^{ii}(\omega,-\boldsymbol{q})]}{d\sigma_{\mathrm{AL}}}\right]^2_{\omega=0}. \tag{55}$$

The explicit calculation of the $\mathcal{R}$ is provided in Appendix D; using the dimensionless function $\mathcal{F}(\boldsymbol{Q}=\boldsymbol{q}\xi_0/\sqrt{\epsilon})$ and substituting bare value of conductivity given by Eq. (32), we arrive at the following general expression:

$$K(\boldsymbol{q}) = \frac{28\zeta(3)}{\pi^2 s_d^2}\frac{1}{\nu_0 T\epsilon^2}\mathcal{F}^2(\boldsymbol{Q}). \tag{56}$$

The relative scale of spatial fluctuations of the conductivity is thus given by $K(\mathbf{r}=0)$. Both asymptotics (D6) and (D9) (for $d=2$ and 3, respectively) show that the integral that defines $K(\mathbf{r}=0)$ is convergent; finally, it yields

$$K(\boldsymbol{r}=0) = \frac{c_d}{\nu_0 T\epsilon^{2-d/2}\xi_0^d}, \tag{57}$$

with the prefactor c, which can be obtained numerically:

$$c_d = \frac{28\zeta(3)}{\pi^2 s_d^2}\int\frac{d^d\boldsymbol{Q}}{(2\pi)^d}\mathcal{F}^2(\boldsymbol{Q}) = \begin{cases}0.141, & (2\mathrm{D})\\ 0.049, & (3\mathrm{D}).\end{cases} \tag{58}$$

Now, let us discuss the obtained result. The Aslamazov-Larkin formula (33) works only provided the correction $K(\mathbf{r}=0) \ll 1$. The result is essentially the same as the one obtained in the previous section: the correction is small provided Eq. (51) holds.

VI. CONCLUSIONS

We have shown in this paper that the fluctuational conductivity effect, originally predicted by Aslamazov and Larkin 50 years ago, remains nearly the same in the case of strongly pseudogapped superconductors with just absent single-electron density of states. The role of single-electron states is taken over by the localized electron pairs, and the effect of that replacement reduces just to the factor-of-2 change of the numerical coefficient s_d in Eqs. (32) and (33) with respect to to the classical Aslamazov-Larkin result, while power-law dependence of paraconductivity on $\epsilon = \ln(T/T_c)$ remains the same. Our results were derived under the assumption that hopping of (initially) localized pairs occurs with a large effective "coordination number" $Z \sim \rho^{-1}$ [see Eqs. (38) and (39)].

The universal character of the AL paraconductivity (especially in 2D) makes it a convenient experimental tool for determination of the critical temperature when $R(T)$ dependence is of considerable width, like it occurs in strongly disordered superconductors. For this reason, the issue of universality of the value of numerical coefficient s_d is of interest. First, we note that it does not depend upon the shape of the local energy distribution function $P(\varepsilon)$ as long as it is flat on the scale of very small $\varepsilon \sim T_c$. Some nontrivial structure at this energy scale in the effective distribution $P(\varepsilon)$ may come about in the generalized model where long-range interaction of the type of $S_i^z U(\boldsymbol{r}_i-\boldsymbol{r}_j)S_j^z$ is included, that can be traced back to the Coulomb interaction between charges of localized pairs. The effect of such an interaction will be studied separately.

Since our condition of a very large pseudogap $\Delta_P \gg T_c$ may be found too restrictive in applications, one might be interested in generalization of our result for moderate value of $\Delta_P \sim T_c$. That can be done in a rather straightforward way, once we note that the whole issue of the coefficient s_d in Eq. (33) is controlled by the expansion of the effective spin distribution function $\mathfrak{f}(\omega) = \tanh\beta\omega$ over small ω. In the standard TDGL theory [23] for disordered superconductors, the fermionic distribution function $f(\omega) = \tanh\frac{\beta\omega}{2}$ stays instead of $\mathfrak{f}(\omega)$, thus making the coefficient in front of $T\tau$ twice smaller than in our problem [see Eq. (27)]. For the general case of $\Delta_P \sim T_c$, we can use an observation presented in Appendix B to the paper [2]: for an arbitrary Δ_P/T, a generalized distribution function is

$$\mathfrak{f}(\omega,\Delta_P) = \frac{\sinh\beta\omega}{\cosh\beta\omega + e^{-\Delta_P/T}}$$

which interpolates between $\tanh\frac{\beta\omega}{2}$ and $\tanh\beta\omega$ upon increase of Δ_P/T. As a result, for generic Δ_P values, the enhancement factor in s_d, with respect to the standard AL result, is given by $2/(1+e^{-\Delta_P/T_c})$, i.e., it quickly becomes close to 2 for moderate $\Delta_P/T \geqslant 1.5$.

All the above discussions refer to the Gaussian fluctuation region $\epsilon \geqslant \epsilon_1$ [see Eqs. (38) and (39)]. At smaller ϵ, nonlinear corrections to the dynamics of the order parameter become important; they are discussed in Sec. IV. However, we present the arguments that power-law character of $\sigma_{\mathrm{AL}}(\epsilon)$ dependence

is not changed due to these "local noise" effects, while the coefficient s_d becomes somewhat different. Even more close to T_c, at $\epsilon \leqslant \epsilon_2 = \mathrm{Gi}$, all types of fluctuational corrections become relevant, which makes calculation of $\sigma_{\mathrm{AL}}(\epsilon)$ difficult. Moreover, in this close proximity of T_c, conductivity becomes spatially inhomogeneous, as evidenced by Eq. (57).

A specific feature of fluctuational conductivity in superconductors close to superconductor-insulator transition is that it may much exceed bare (unrelated to superconducting correlations) conductivity already in the region of $\epsilon \geqslant \epsilon_1$ where Gaussian approximation is valid. This is due to the absence in our case of the standard Drude contribution of the normal-metal type. Instead, Aslamazov-Larkin paraconductivity competes with hopping conductivity of individual electrons, that is further suppressed at $T \ll \Delta_P$. Finally, we mention again that the AL effect is the only fluctuational contribution to conductivity in a pseudogapped superconductor. In particular, it makes possible to account for nonlinear (in applied electric field) effects, using the approach [25] applicable for any TDGL-type theory.

ACKNOWLEDGMENTS

We are grateful to L. Ioffe for useful discussions. This research was partially supported by the Russian Science Foundation Grant No. 14-42-00044, by the Basic research program of the HSE, and by a grant from the Basis Foundation (I.P.) supported by Skoltech NGP Program (Skoltech-MIT joint project).

APPENDIX A: MEAN FIELD APPROXIMATION AND FINITE R EFFECTS ON T_c

This Appendix is devoted to analytical and numerical study of the critical temperature T_c at the mean field level. In Sec. II A we have formulated the following condition for the appearance of order parameter: the largest eigenvalue of the matrix $J_{ij}\sqrt{\eta_i \eta_j}$ should be larger than unity. This criterion was then solved in the limit $R \to \infty$ yielding Eq. (7). Here, we consider leading corrections to this result at large R.

We start our analysis with analytical treatment of the spectrum (DOS) of matrix $J_{ij}\sqrt{\eta(\varepsilon_i)\eta(\varepsilon_j)}$, averaged over the distribution $P(\varepsilon)$. For this purpose, we express the DOS in terms of Green function $\hat{G}_E = (E - \hat{\eta}^{1/2}\hat{J}\hat{\eta}^{1/2} + i0)^{-1}$ as $\nu(E) = -\frac{1}{\pi N}\,\mathrm{Tr}\,\hat{G}_E$, and expand it in Dyson series. The latter can be rewritten more conveniently in terms of auxiliary matrix $\hat{F}_E = \hat{\eta}^{-1/2}\hat{G}_E\hat{\eta}^{1/2}\hat{J}$:

$$\hat{F}_E = \hat{F}_E^{(0)} + \hat{F}_E^{(0)}\hat{\eta}\hat{F}_E^{(0)} + \hat{F}_E^{(0)}\hat{\eta}\hat{F}_E^{(0)}\hat{\eta}\hat{F}_E^{(0)} + \cdots, \tag{A1}$$

with $\hat{F}_E^{(0)} = \hat{J}/(E + i0)$. Under the assumption of large radius R, we can apply an ordinary impurity diagram technique utilizing the equation $\langle \eta_i \eta_j \rangle = \delta_{ij}\langle \eta^2 \rangle + (1 - \delta_{ij})\langle \eta \rangle^2$. The first approximation for the self-energy corresponds to trivial mean field analysis performed in Sec. II A and reads as $\hat{\Sigma}^{(1)} = \langle \eta \rangle$. In order to study the DOS near the spectrum edge, we utilize the self-consistent Born approximation (SCBA) and consider the following self-energy correction:

$$\hat{\Sigma}^{(2)} = \langle\langle \eta^2 \rangle\rangle \cdot (\hat{F}_E)_{ii}. \tag{A2}$$

In the momentum representation, the Dyson equation for the SCBA then reads as

$$F_E^{-1}(\boldsymbol{q}) = J(\boldsymbol{q})^{-1}(E + i0) - \langle \eta \rangle - \langle\langle \eta^2 \rangle\rangle F(E), \tag{A3}$$

with $F(E) = \int (d\boldsymbol{q}) F_E(\boldsymbol{q})$. This allows us to write a single self-consistency equation for $F(E)$:

$$F(E) = \int \frac{d^d \boldsymbol{q}/(2\pi)^d}{J^{-1}(\boldsymbol{q})(E + i0) - \langle \eta \rangle - \langle\langle \eta^2 \rangle\rangle F(E)}. \tag{A4}$$

The next step is to express the density of states in terms of the function $F(E)$. First, we note that $\hat{G}_E = \hat{\eta}^{1/2}\hat{F}_E\hat{J}^{-1}\hat{\eta}^{-1/2}$, and thus $\mathrm{Tr}\,\hat{G}_E = \mathrm{Tr}(\hat{F}_E\hat{J}^{-1})$. In the UV limit $q \to \infty$ we have $J(\boldsymbol{q}) \to 0$, which leads to the delta peak at zero energy. Since we are studying the edge of the spectrum, we can subtract the value $(E + i0)^{-1}$ and focus at $E > 0$. Utilizing then the equation for $F(E)$, we obtain the following general expression for the DOS:

$$\nu(E > 0) = -\frac{1}{\pi E}\mathrm{Im}(F(E)[\langle \eta \rangle + \langle\langle \eta^2 \rangle\rangle F(E)]). \tag{A5}$$

We now proceed with solving Eq. (A4). We switch to dimensionless momentum $Q = qR$ and dimensionless variables:

$$\lambda = \frac{E}{J\langle \eta \rangle} - 1, \quad \Psi(\lambda) = F(E)\langle \eta \rangle R^d, \quad j(\boldsymbol{Q}) = J(\boldsymbol{q})/J, \tag{A6}$$

leaving us with the single small dimensionless parameter, which controls the SCBA:

$$\alpha = \frac{\langle\langle \eta^2 \rangle\rangle}{R^d t \langle \eta \rangle^2} = \frac{1}{R^d}\left[\frac{14\zeta(3)}{\pi^2}\frac{\beta W}{\ln^2 \frac{4e^\gamma \beta W}{\pi}} - 1\right] \sim \frac{g^2 e^{1/g}}{R^d} \ll 1. \tag{A7}$$

The dimensionless form of Eq. (A4) then reads as

$$\Psi(\lambda) = \int \frac{d^d \boldsymbol{Q}/(2\pi)^d \cdot j(\boldsymbol{Q})}{\lambda + i0 + 1 - j(\boldsymbol{Q}) - \alpha j(\boldsymbol{Q})\Psi(\lambda)}, \tag{A8}$$

and DOS is expressed in terms of Ψ function as follows:

$$\nu(E) = -\frac{1}{\pi E R^d}\mathrm{Im}[\Psi(\lambda) + \alpha\Psi^2(\lambda)]. \tag{A9}$$

The long-wavelength limit $j(\boldsymbol{Q}) = 1 - Q^2$ is sufficient for the study of the DOS behavior near the spectrum edge $E \approx J\langle \eta \rangle$, that is, $|\lambda| \ll 1$. Performing momentum expansion and focusing for the sake of simplicity on the 2D case, where the integral is logarithmic, we arrive at the following equation:

$$\Psi(\lambda) \approx \frac{1}{4\pi}\ln\frac{c}{\lambda + i0 - \alpha\Psi(\lambda)}, \tag{A10}$$

where c is a constant of order of unity depending on the UV behavior of $j(\boldsymbol{Q})$. In the limit $R \to \infty$, that is $\alpha = 0$, this equation leads to the steplike DOS with the sharp edge at $\lambda = 0$, $\nu(E) \approx \theta(J\langle \eta \rangle - E)/4\pi R^2$. Finite but small α rounds out the step leading to the square-root singularity at the slightly shifted edge:

$$\nu(E) \approx \frac{1}{\pi E R^d}\sqrt{\frac{\lambda_G - \lambda}{2\pi\alpha}}, \tag{A11}$$

with

$$\lambda_G = \frac{\alpha}{4\pi}\ln\frac{4\pi ec}{\alpha}. \tag{A12}$$

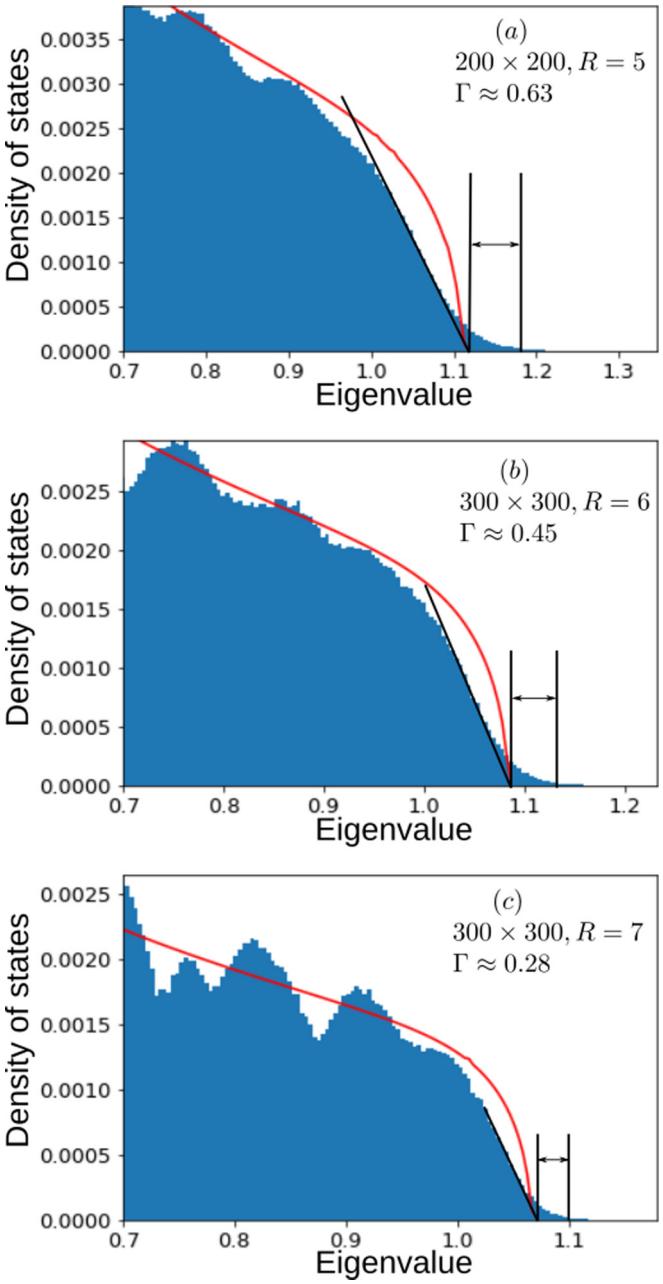

FIG. 9. DOS $\nu(E)$ for 2D system with parameters $W = 3$, $J = 1$, which corresponds by Eq. (7), $T_c^{-1} \approx 60$. Red curve: solution of the SCBA equation (A8) and substituting the solution to (A9).

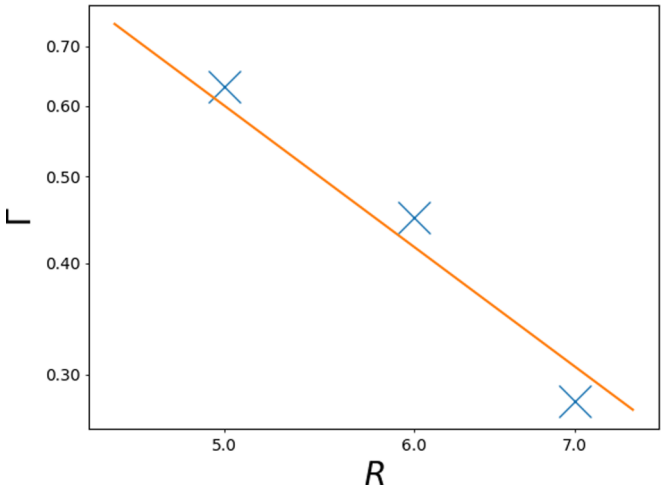

FIG. 10. R dependency of the width of the tail extracted from Fig. 9. Line corresponds to R^{-2}.

The shift of the spectrum edge leads to the renormalization of the coupling constant $J_{\text{eff}} = J(1 + \lambda_G)$ in the expression for T_c [Eq. (7)], thus increasing the critical temperature slightly.

To support this calculation, we have performed numerical analysis of the spectrum of corresponding random matrix. The temperature $T = \beta^{-1}$ was taken close to the mean field value of the critical temperature (7), so that the spectrum edge is estimated to be close to unity. The J_{ij} matrix was taken Gaussian, so that its Fourier transform has the form $J(\boldsymbol{q}) = J\exp(-q^2R^2)$; in that case, the integration in Eq. (A8) can be performed explicitly, leaving the single algebraic equation for Ψ, which is then solved numerically to obtain the analytic fitting curve. The amount of disorder realization varied from ∼30 000 (for the smallest system) to ∼6000 for the largest one.

The typical DOS pictures shown on Fig. 9 consists of the "main body" of the DOS, which is fitted by the SCBA formula reasonably well, and the exponential tail of localized states which always arises when one deals with random matrices. The oscillatory behavior is due to finite-size effects and momentum quantization in a system of finite size; they tend to increase upon increasing R and decreasing L. The superconductivity appears when the mobility edge separating localized and delocalized states crosses unity eigenvalue. Clearly, the edge of the spectrum is larger than unity, and the SCBA result (A11) gives the better estimation of the position of the edge as well as the whole curve.

The width of the tail Γ is known to be related to the Ginzburg number $\text{Gi} \sim \rho^{2/(4-d)} \propto R^{-2d/(4-d)}$. To support this claim, we performed numerical simulations for system with various R and estimated the R dependency of the width of the tail. The beginning of the tail was determined by the intersection of the tangent line to the curve in the inflection point with the x axis (see Fig. 9). The end of the tail was chosen as the point where the DOS value is equal to 4×10^{-5}. The best fit of the $\Gamma(R)$ dependency is shown on Fig. 10, and corresponds to $\Gamma(R) \sim R^{-2}$, which agrees with the prediction for $d = 2$.

APPENDIX B: KELDYSH DIAGRAM TECHNIQUE FOR PSEUDOSPINS

In this Appendix we will derive the Keldysh action and rules for diagram technique used to describe the pseudospin model (2) and its semionic representation (10) following Kiselev and Opperman [26]. We introduce the standard Keldysh time contour $C = (-\infty,\infty) \cup (\infty,-\infty)$ for the model and introduce the following action for the semions:

$$iS[\bar\psi,\psi] = i\int_C dt\left(\bar\psi\hat G^{-1}\psi + \frac{1}{4}(\bar\psi\hat\sigma^\alpha\psi)\hat J(\bar\psi\hat\sigma^\alpha\psi)\right), \quad \text{(B1)}$$

where $\hat G^{-1} = i\partial_t + \varepsilon_i\sigma^z$ is the diagonal matrix in real space, and implied summation over coordinates. We introduce the two-component real Hubbard-Stratanovich field $\Phi = (\Phi^x,\Phi^y)$

with the following action:

$$iS[\Phi] = -i\int_C dt\ \Phi^\alpha \hat{J}^{-1}\Phi^\alpha, \tag{B2}$$

and perform a shift to decouple four-semion interaction $\Phi^\alpha \mapsto \Phi^\alpha - \frac{1}{2}\hat{J}\bar{\psi}\sigma^\alpha\psi$, arriving at following action:

$$iS[\bar{\psi},\psi,\Phi] = i\int_C dt(-\Phi^\alpha \hat{J}^{-1}\Phi^\alpha + \bar{\psi}(\hat{G}^{-1} + \hat{\sigma}^\alpha\Phi^\alpha)\psi). \tag{B3}$$

This action effectively describes spin-$\frac{1}{2}$ lying in a fluctuating magnetic field $(\Phi_i^x(t),\Phi_i^y(t),\varepsilon_i)$, whose dynamics itself is coupled to the spins via the interaction vertex. This is thus a clear generalization of a simple static mean field model described in Sec. II A.

The next step is to separate fields lying on the upper and lower parts of the Keldysh contour as $\Phi = (\Phi_+,\Phi_-)$ (and similarly for ψ), and introduce a Keldysh rotation switching to "classical" and "quantum" bosonic fields: $\Phi' = (\Phi_{cl},\Phi_q)$; and their analog for fermions: $\psi' = (\psi_1,\psi_2)^T$, $\bar{\psi}' = (\bar{\psi}_1,\bar{\psi}_2)$, via the following relations:

$$\Phi = \check{O}\Phi', \quad \psi = \check{O}\psi', \quad \bar{\psi} = \bar{\psi}'\check{O}\check{\tau}_z, \tag{B4}$$

with matrix $\check{O} = (\check{\tau}_x + \check{\tau}_z)/\sqrt{2}$ and $\check{\tau}_\alpha$ being Pauli matrices acting in Keldysh space. This rotation yields following Keldysh structure of the propagators:

$$\check{L} = i\langle\Phi\Phi^T\rangle = \begin{pmatrix} L_K & L_R \\ L_A & 0\end{pmatrix}, \tag{B5}$$

$$\check{G} = -i\langle\psi\bar{\psi}\rangle = \begin{pmatrix} G_R & G_K \\ 0 & G_A\end{pmatrix}. \tag{B6}$$

Finally, the "rotated" action is given by Eq. (11). In principle, one can perform Gaussian integration over semionic degrees of freedom and obtain the effective action describing only the order-parameter dynamics:

$$iS[\Phi] = -i\int dt\ \Phi^\alpha \hat{J}^{-1}\check{\tau}_x\Phi^\alpha + \mathrm{Tr}\ln\left(\hat{G}^{-1} + \frac{1}{\sqrt{2}}\check{\Gamma}_i\hat{\sigma}^\alpha\Phi_i^\alpha\right). \tag{B7}$$

We remind that the order-parameter fields $\Phi \equiv \Phi_\mu^\alpha(\boldsymbol{r}_i)$ have the following indices: "spin space" $\alpha \in (x,y)$, Keldysh space $\mu \in (cl,q)$, and real space $\boldsymbol{r}_i$, while the semionic fields $\psi \equiv \psi_{\sigma,\mu}(\boldsymbol{r}_i)$ reside in "semionic pseudospin space" $\sigma \in \{\uparrow,\downarrow\}$, Keldysh space $\mu \in \{1,2\}$, and real space $\boldsymbol{r}_i$.

APPENDIX C: "IMPURITY" DIAGRAM TECHNIQUE

The aim of this Appendix is to develop an "impuritylike" diagram technique which is used in Sec. V to study the deviations from the mean field approximation presented in Sec. III due to the averaging over the distribution of $\{\varepsilon_i\}$. The key element of the diagram technique that depended on the ε is the "crossed circle" presented on Fig. 2, which represents spin-correlation function $S_R^{\alpha\beta}(\omega)$. Upon averaging the, e.g., Dyson series (17), the next nontrivial object arising is simultaneous averaging of two spin-correlation functions corresponding to the single site $\langle S_R^{\alpha\mu}(\omega_1)S_R^{\nu\beta}(\omega_2)\rangle_\varepsilon$, which corresponds to the "impurity line" connecting two crossed circles in our diagram technique.

We proceed with the calculation of analytic expression for "impurity line" utilizing the spin structure (21) and expressions (22) and (23). The cross term $\langle S_R^{(\mathrm{diag})}(\omega_1)S_R^{(\mathrm{off})}(\omega_2)\rangle_\varepsilon$ drops out due to its parity, while nonzero terms for $\omega_{1,2} \ll T$ yield

$$\begin{aligned}\left\langle S_R^{(\mathrm{diag})}(\omega_1)S_R^{(\mathrm{diag})}(\omega_2)\right\rangle_\varepsilon &= \left\langle \frac{\mathfrak{f}^2(\varepsilon)\varepsilon^2}{[(\omega_1/2+i0)^2-\varepsilon^2][(\omega_2/2+i0)^2-\varepsilon^2]}\right\rangle_\varepsilon \\ &\approx \frac{14\zeta(3)}{\pi^2 WT} + \frac{i\pi}{4WT^2}\frac{\omega_1^2+\omega_2^2+\omega_1\omega_2}{\omega_1+\omega_2+i0},\end{aligned} \tag{C1}$$

$$\begin{aligned}\left\langle S_R^{(\mathrm{off})}(\omega_1)S_R^{(\mathrm{off})}(\omega_2)\right\rangle_\varepsilon &= \frac{\omega_1\omega_2}{4}\left\langle \frac{\mathfrak{f}^2(\varepsilon)}{[(\omega_1/2+i0)^2-\varepsilon^2][(\omega_2/2+i0)^2-\varepsilon^2]}\right\rangle_\varepsilon \\ &\approx \frac{i\pi}{4WT^2}\frac{\omega_1\omega_2}{\omega_1+\omega_2+i0}.\end{aligned} \tag{C2}$$

APPENDIX D: CALCULATION OF CONDUCTIVITY CORRELATION FUNCTION

Here, we briefly discuss the calculation of the conductivity fluctuations $\langle\delta\sigma(\boldsymbol{r},\boldsymbol{x})\delta\sigma(\boldsymbol{r}',\boldsymbol{y})\rangle$ in the lowest order of perturbation theory given by the diagram shown on Fig. 8. The analytic expression for the loop integrals $\mathcal{R}^{ij}$ appearing in Sec. V B reads as follows:

$$\begin{aligned}\mathcal{R}^{ij}(\omega,\boldsymbol{q}) = i\frac{8\xi_0^4}{W^2}\int\frac{d\Omega}{2\pi}\frac{d^d\boldsymbol{p}}{(2\pi)^d}p^i p_+^j[&\mathfrak{B}(\Omega_-)L_R(\Omega_+,\boldsymbol{p}_+)[L_R(\Omega_-,\boldsymbol{p}_+)L_R(\Omega_-,\boldsymbol{p}_-) - L_A(\Omega_-,\boldsymbol{p}_+)L_A(\Omega_-,\boldsymbol{p}_-)] \\ &+ \mathfrak{B}(\Omega_+)[L_R(\Omega_+,\boldsymbol{p}_+) - L_A(\Omega_+,\boldsymbol{p}_+)L_A(\Omega_-,\boldsymbol{p}_+)L_A(\Omega_-,\boldsymbol{p}_-)]].\end{aligned} \tag{D1}$$

In the low-frequency limit, we take $\mathfrak{B}(\Omega) \approx 2T/\Omega$, and perform integration over energy Ω using residues, arriving at

$$\mathcal{R}^{ij}(\omega,\boldsymbol{q}) = 16WT\xi_0^4\int\frac{d^d\boldsymbol{p}}{(2\pi)^d}p^i p_+^j\frac{\epsilon + (\boldsymbol{p}^2+\boldsymbol{q}^2/4)\xi_0^2 - i\omega\tau/4}{(\epsilon+\boldsymbol{p}_-^2\xi_0^2)(\epsilon+\boldsymbol{p}_+^2\xi_0^2)(\epsilon+\boldsymbol{p}_+^2\xi_0^2-i\omega\tau/2)[\epsilon+(\boldsymbol{p}^2+q^2/4)\xi_0^2-i\omega\tau/2]}. \tag{D2}$$

This integral is taken at finite external momentum and thus it can have nontrivial tensor structure. We are interested in the diagonal conductivity, which is $\delta\sigma = \frac{1}{d}\sigma^{ii}$. The next step is to make momentum integration dimensionless introducing $\boldsymbol{P} = \boldsymbol{p}\xi_0/\sqrt{\epsilon}$,

expand it in frequency, take trace $\mathcal{R}^{ii}/d \equiv \mathcal{R}$, and introduce dimensionless function $\mathcal{F}(\boldsymbol{Q})$:

$$i\partial_\omega \mathcal{R}(\omega=0,\boldsymbol{Q}) = -\frac{W}{\xi_0^{d-2}\epsilon^{3-d/2}}\frac{\pi}{d}\int\frac{d^d\boldsymbol{P}}{(2\pi)^d}\frac{\boldsymbol{P}^2+\boldsymbol{P}\boldsymbol{Q}/2}{(1+\boldsymbol{P}_-^2)(1+\boldsymbol{P}_+^2)^2}\left(\frac{1}{1+P^2+\boldsymbol{Q}^2/4}+\frac{2}{1+\boldsymbol{P}_+^2}\right) \equiv -\frac{W}{\xi_0^{d-2}\epsilon^{3-d/2}}\mathcal{F}(\boldsymbol{Q}). \quad \text{(D3)}$$

We now switch to the calculation of this function in arbitrary spatial dimensionality.

a. 2D case. Using substitution $a = 1+P^2+Q^2/4$, we perform angular averaging, arriving at

$$\mathcal{F}(\boldsymbol{Q}) = \frac{1}{16}\int_0^\infty P^3 dP\,\frac{12a^4+Q^2(2P^2Q^2-5a^2)(a+2P^2)}{a^3(a^2-P^2Q^2)^{5/2}}. \quad \text{(D4)}$$

Finally, we integrate over momentum; using substitution $Q = 2\sinh\theta$, the integral yields

$$\mathcal{F}(Q=2\sinh\theta) = \frac{1}{64\cosh^2\theta}\left(1+3\frac{2\theta}{\sinh 2\theta}\right), \quad \text{(D5)}$$

with the following asymptotic behavior:

$$\mathcal{F}(Q) \approx \frac{1}{16}\cdot\begin{cases}1, & Q\ll 1\\ 1/Q^2, & Q\gg 1\end{cases} \quad \text{(2D)}. \quad \text{(D6)}$$

b. 3D case. We use the same substitution $a = 1+P^2+Q^2/4$, and angular averaging yields

$$\mathcal{F}(\boldsymbol{Q}) = \frac{1}{12\pi}\int_0^\infty dP\,\frac{P}{a^3}\left[\frac{a+2P^2}{Q}\operatorname{arctanh}\frac{PQ}{a} - \frac{aP(a^3-4a^2P^2+2P^4Q^2)}{(a^2-P^2Q^2)^2}\right]. \quad \text{(D7)}$$

Again, using the same substitution $Q = 2\sinh\theta$, the integral yields

$$\mathcal{F}(Q=2\sinh\theta) = \frac{1}{192\cosh^2\theta}\left(2+\frac{1}{\cosh^2(\theta/2)}\right), \quad \text{(D8)}$$

with the following asymptotic behavior:

$$\mathcal{F}(Q) \approx \frac{1}{192}\cdot\begin{cases}3, & Q\ll 1\\ 8/Q^2, & Q\gg 1\end{cases} \quad \text{(3D)}. \quad \text{(D9)}$$

[1] M. V. Feigel'man, L. B. Ioffe, V. E. Kravtsov, and E. A. Yuzbashyan, Phys. Rev. Lett. **98**, 027001 (2007).

[2] M. V. Feigel'man, L. B. Ioffe, V. E. Kravtsov, and E. Cuevas, Ann. Phys. (NY) **325**, 1390 (2010).

[3] G. Lemarié, A. Kamlapure, D. Bucheli, L. Benfatto, J. Lorenzana, G. Seibold, S.C. Ganguli, P. Raychaudhuri, and C. Castellani, Phys. Rev. B **87**, 184509 (2013).

[4] Y. L. Loh, M. Randeria, N. Trivedi, C.-C. Chang, and R. Scalettar, Phys. Rev. X **6**, 021029 (2016).

[5] B. Sacépé, Th. Dubouchet, C. Chapelier *et al.*, Nat. Phys. **7**, 239 (2011).

[6] B. Sacépé, C. Chapelier, T. I. Baturina, V. M. Vinokur, M. R. Baklanov, and M. Sanquer, Phys. Rev. Lett. **101**, 157006 (2008).

[7] S. P. Chockalingam, M. Chand, A. Kamlapure, J. Jesudasan, A. Mishra, V. Tripathi, and P. Raychaudhuri, Phys. Rev. B **79**, 094509 (2009).

[8] G. Sambandamurthy, L. W. Engel, A. Johansson, and D. Shahar, Phys. Rev. Lett. **92**, 107005 (2004).

[9] M. Ovadia, B. Sacépé, and D. Shahar, Phys. Rev. Lett. **102**, 176802 (2009).

[10] V. F. Gantmakher and V. T. Dolgopolov, Phys. Usp. **53**, 1 (2010).

[11] A. Goldman and N. Markovic, Phys. Today **51**(11), 39 (1998).

[12] M. Chand, G. Saraswat, A. Kamlapure, M. Mondal, S. Kumar, J. Jesudasan, V. Bagwe, L. Benfatto, V. Tripathi, and P. Raychaudhuri, Phys. Rev. B **85**, 014508 (2012).

[13] E. F. C. Driessen, P. C. J. J. Coumou, R. R. Tromp, P. J. de Visser, and T. M. Klapwijk, Phys. Rev. Lett. **109**, 107003 (2012).

[14] Th. Dubouchet, Ph.D. thesis, Neel Institute, Grenoble, 2010.

[15] M. Ma and P. A. Lee, Phys. Rev. B **32**, 5658 (1985).

[16] A. Ghosal, M. Randeria, and N. Trivedi, Phys. Rev. B **65**, 014501 (2001).

[17] L. G. Aslamazov, A. I. Larkin, Sov. Phys.–Solid State **10**, 875 (1968)[Fiz. Tverd. Tela **10**, 1104 (1968)].

[18] A. Z. Patashinskii and V. L. Pokrovskii, *Fluctuation Theory of Phase Transitions* (Pergamon, Oxford, 1979).

[19] A. I. Larkin and Yu. N. Ovchinnikov, Zh. Eksp. Teor. Fiz. **119**, 595 (2001) A. I. Larkin and Yu. N. Ovchinnikov, [JETP **92**, 519 (2001)].

[20] P. W. Anderson, Phys. Rev. **112**, 1900 (1958).

[21] V. N. Popov and S. A. Fedotov, Zh. Eksp. Teor. Fiz. **94**, 183 (1988) [JETP **67**, 535 (1988)].

[22] A. V. Shtyk and M. V. Feigel'man, Phys. Rev. B **96**, 064523 (2017).

[23] A. Larkin and A. Varlamov, *Theory of Fluctuations in Superconductors* (Oxford University Press, Oxford, 2005).

[24] L. D. Landau and E. M. Lifshitz, *Electrodynamics of Continuous Media* (Vol. 8 of a Course of Theoretical Physics) (Pergamon, Oxford, 1960), Chap. 2.

[25] T. Mishonov, A. Posazhennikova, and J. Indekeu, Phys. Rev. B **65**, 064519 (2002).

[26] M. N. Kiselev and R. Oppermann, Phys. Rev. Lett. **85**, 5631 (2000).